UNIVERSITA' DI NAPOLI FEDERICO II

DOTTORATO DI RICERCA
BIOCHIMICA E BIOLOGIA CELLULARE E MOLECOLARE
XXV CICLO

Ribonuclease/angiogenin inhibitor 1 and angiogenin: regulation of their intracellular localization in stress response

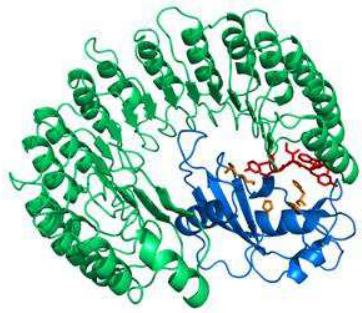

Candidate
Carmen Sarcinelli

Tutor
Dott. Eliodoro Pizzo

Coordinator
Prof. Paolo Arcari

Academic Year 2012/2013

Riassunto

Lo stress cellulare, indotto da fattori xenobiotici o fisici, generalmente comporta l'attivazione di un programma di risposta integrato, che modifica il metabolismo cellulare allo scopo di preservare l'energia anabolica necessaria ai meccanismi di riparazione del conseguente danno molecolare. Nelle cellule eucariotiche, un evento caratteristico è rappresentato dall'assemblaggio dei granuli da stress, la cui funzione è proteggere le molecole di RNA messaggero represse a livello traduzionale, in seguito alla fosforilazione della subunità α del fattore di inizio della traduzione eIF2. Nella risposta allo stress, particolare rilevanza va sicuramente attribuita al taglio dei tRNA, operato da ribonucleasi (RNasi) stress-indotte che vengono attivate nel citoplasma, tra cui l'angiogenina (ANG). ANG è una ribonucleasi secretoria di circa 14 kDa appartenente alla Superfamiglia delle RNasi da Vertebrati, con differenti proprietà biologiche. In condizioni di crescita, ANG trasloca nel nucleo, accumulandosi particolarmente nei nucleoli dove stimola la trascrizione dell'rRNA e di conseguenza la biogenesi dei ribosomi, promuovendo la crescita cellulare. Nella risposta allo stress, ANG, idrolizzando gli RNA transfer, produce piccoli frammenti denominati tiRNA, che inducono l'arresto della sintesi proteica, e attraverso un *pathway* indipendente dalla fosforilazione di eIF2α, promuovono la formazione dei granuli da stress e quindi la sopravvivenza cellulare. La localizzazione subcellulare di ANG in condizioni di stress e come le sue attività siano regolate nelle differenti condizioni di crescita sono ancora da chiarire. In questo studio è stato dimostrato che in cellule stressate ANG è localizzata nei granuli da stress e che la sua localizzazione e le sue attività sono regolate dall'inibitore delle ribonucleasi (RNH1), con il quale ANG condivide una costante di dissociazione fentomolare. RNH1 è una proteina di circa 50 kDa, ricca in residui di leucina (15 LRR) e cisteina, il cui ruolo fisiologico non è ancora del tutto delineato. In condizioni fisiologiche ANG è maggiormente presente nel nucleo, dove non è associata a RNH1 in modo che ANG possa stimolare la trascrizione dell'rRNA. Al contrario, tracce di ANG a livello citoplasmatico sono inibite da RNH1, per evitare di conseguenza una degradazione incontrollata dell'RNA cellulare. In condizioni di stress ANG lascia il compartimento nucleare per localizzarsi principalmente nel citoplasma, in particolare nei granuli da stress. La distribuzione subcellulare di RNH1 nelle diverse condizioni di crescita è opposta a quella di ANG: in condizioni di stress aumenta il livello nucleare di RNH1, mentre sembra ridursi la sua concentrazione citoplasmatica. Inoltre, dato particolarmente interessante, è risultato che anche RNH1 è reclutato nei granuli da stress. Sebbene sia stato riscontrato che ANG e RNH1 colocalizzano in alcuni granuli da stress, è stato evidenziato che non interagiscono tra loro. Nel

citoplasma di cellule stressate quindi ANG è libera dal legame con RNH1 e, di conseguenza, in grado di esercitare la propria attività enzimatica. Nel nucleo ANG è invece inibita da RNH1, per preservare probabilmente l'energia anabolica necessaria alla cellula. Questi risultati dimostrano che la localizzazione subcellulare di ANG e RNH1 è dinamica e dipende dallo stato di crescita della cellula. Il silenziamento dell'espressione genica di RNH1, mediato da vettori lentivirali, ha permesso di stabilire che RNH1 ha un effetto sulla regolazione dell'attività e della localizzazione di ANG nella cellula. Il silenziamento di RNH1 compromette fortemente la localizzazione di ANG nei granuli da stress favorendone al contempo una maggiore localizzazione nucleolare. Il reale significato della ridistribuzione subcellulare di ANG non è chiaro, tuttavia RNH1 sembra esercitare chiaramente una certa influenza nel movimento intracellulare di ANG nelle diverse condizioni, e quindi le sue proprietà funzionali in condizioni fisiologiche e di stress. E' stato infine evidenziato che l'attenuazione dell'espressione di RNH1 riduce la proliferazione e la sopravvivenza cellulare, probabilmente in seguito a un incremento del livello di apoptosi cellulare.

Summary

Under stress conditions eukaryotic cells activate an integrate response pathway to modulate cell metabolism. A hallmark of the stress response is transient formation of ribonucleo-protein cytoplasmic foci named stress granules (SGs) to protect translationally silenced mRNA. Regard to stress response, notable is the role of angiogenin (ANG), a member of the Vertebrate Ribonuclease Superfamily. Under growth conditions, ANG undergoes nuclear translocation and is accumulated in nucleolus where it stimulates ribosomal RNA (rRNA) transcription. When cells are stressed, ANG mediates the production of cytoplasmic tRNA-derived stress-induced small RNA (tiRNA) that suppress global protein translation and promote cell survival. It is unknown where ANG is localized in stressed cells and how ANG activities are regulated in the cell under different growth conditions. In this study it has been reported that ANG is localized in stress granules (SGs) when cells are stressed and that its localization as well as its activities are regulated by ribonuclease/angiogenin inhibitor 1 (RNH1), that binds ANG with an affinity in femtomolar range. Under growth conditions, ANG is mainly located in the nucleus where it is not associated with RNH1 so that ANG is able to stimulate rRNA transcription. Whereas cytoplasmic ANG traces are associated with RNH1 to avoid accordingly random RNA degradation. Under stress conditions, ANG leaves nuclear compartment to become mainly localized in the cytoplasm especially concentrated in SGs. Extremely intriguing, although RNH1 is also recruited to SGs, RNH1 and ANG are not physically associated in SGs so that ANG is able to keep its enzymatic activity. In contrast, nuclear ANG traces are inhibited by RNH1 in stressed cells maybe to preserve anabolic energy needed to the cell. Subcellular distribution pattern of RNH1 under different growth conditions is opposite. Under stress conditions, RNH1 is accumulated in nuclear compartment, whereas its cytoplasmic level is reduced and in the same time it is also recruited to SGs. These results demonstrate that subcellular localization of ANG and RNH1 is dynamic and dependent on the growth status of the cell. Moreover, knockdown of RNH1 abolishes stress-induced localization of ANG to SGs and decrease cell survival under stress so that RNH1 regulates ANG localization in both growth and stress conditions and control growth and survival behaviours.

Index

List of Figures

Abbreviations

SG	Stress Granule
ANG	Angiogenin
RNH1	RiboNuclease/angiogenin inHibitor 1
PABP	Poly(A)-Binding Protein
RPS3	40S Ribosomal Protein S3
PCNA	Proliferating Cell Nuclear Antigen
IgG	ImmunoGlobulin G
mAb	Monoclonal AntiBody
pAb	Policlonal AntiBody
OD	Optical Density
Rpm	rivolutions per minute
shRNA	short hairpin RNA
FRET	Fluorescence Resonance Energy Transfer
FBS	Fetal Bovine Serum
DMEM	Dulbecco's Modified Eagle Medium
RPMI	Roswell Park Memorial Institute medium
SDS	Sodium Dodecyl Sulfate
SDS-PAGE	SDS-PolyAcrylamide Gel Electrophoresis
BSA	Bovine Serum Albumin
NP-40	Nonidet P-40
RIPA buffer	RadioImmunoPrecipitation Assay buffer
PBS	Phosphate Buffered Saline
TRIS	Tris [hydroxymethyl] aminomethane
HEPES	Acid 4-2-HydroxyEthyl-1-Piperazinyl-EthaneSulfonic
EDTA	EthyleneDiamineTetraAcetate
SA	Sodium Arsenite
DTT	DiThioThreitol
PVDF	PolyVinylidene DiFluoride
EB	Ethidium Bromide
AO	Acridine Orange

1.Introduction

1.1 The cell stress response

The cellular response to environmental stress, caused by xenobiotics or physical factors, involves an integrated response program that modifies the cell metabolism. To conserve anabolic energy needed to the efficient repair of stress-induced molecular damage, eukaryotic cells activate a radical and rapid reprogramming of ongoing translation. So, they strongly reduce the expression of housekeeping genes, while increase the expression of genes that repair stress-induced damage as genes encoding heat shock proteins and some transcription factors. Multiple and parallel mechanisms have evolved to modulate protein synthesis, in adverse environmental conditions, targeting both protein and RNA components of the translation machinery (Yamasaki and Anderson, 2008).

The major event in the global stress response pathway, that affects the translation machinery, is represented by the phosphorylation of the α-subunit of the general translation initiation factor eIF2 by a family of serine/threonine kinases, sensors of environmental stress (Kimball et al., 2003). Stress-induced phosphorylation of eIF2α results in a depletion of active eIF2-GTP-$tRNA_i^{Met}$ ternary complexes and thus the inhibition of translation initiation (Figure 1.1). However, data regarding the arrest of ongoing protein synthesis in cells expressing a non-phosphorilable eIF2α have been reported, indicating an alternative pathway of translational control (McEwen et al., 2005).

Phosphorylation of eIF2α and the subsequent depletion of active eIF2-GTP-$tRNA_i^{Met}$ ternary complexes induce mRNAs encoding housekeeping proteins to aggregate in cytoplasmic foci named stress granules (SGs) (Figure 1.2).

The transient formation of SGs was recently reported to be a hallmark of the stress response (heat, UV irradiation, oxidative stress but no X-ray) to preserve a subset of translationally silenced mRNAs (Kedersha and Anderson, 2002), found in both cultured cell lines and intact tissues.

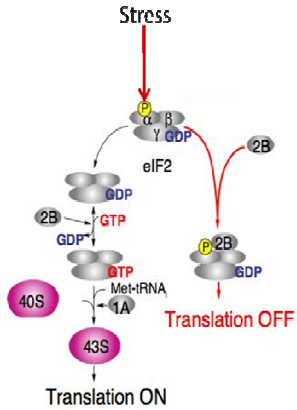

Figure 1.1 Phosphorylation of the α-subunit of eukaryotic initiation factor 2 (eIF2) causes protein synthesis arrest in stressed cells.

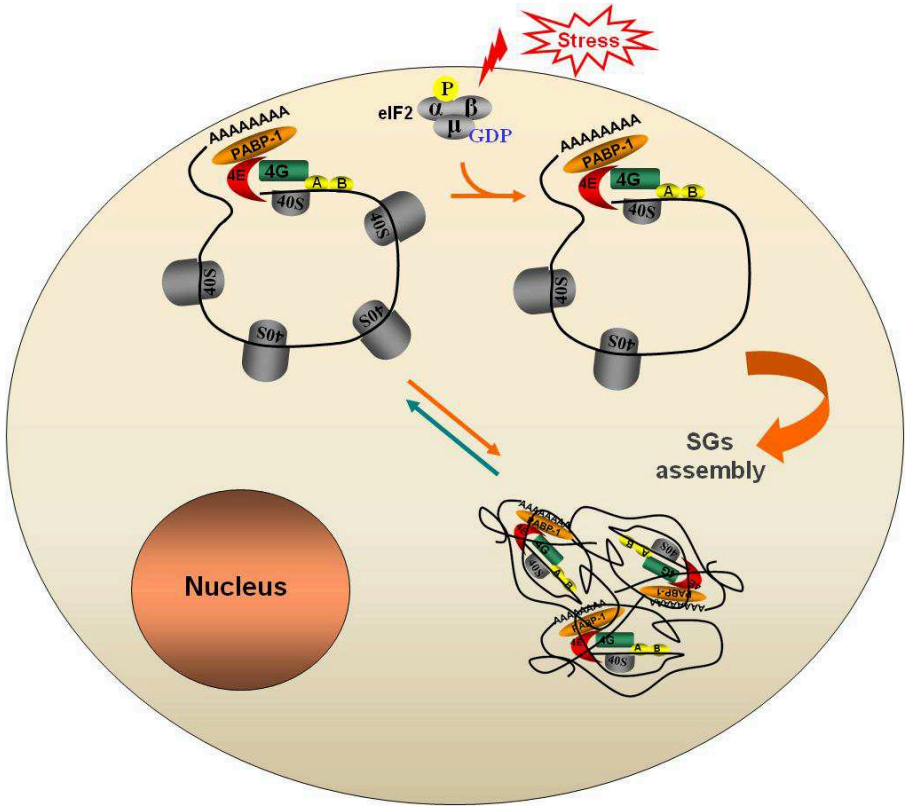

Figure 1.2 Model of SG assembly in the cell during stress (personal adjustment).

Following the phosphorylation of eIF2α and reduced availability of the ternary complexes, eIF2/eIF5-deficient pre-initiation complexes and their associated mRNAs (stalled 48S pre-initiation complexes) participate in the assembly of SGs. SGs are formed as translating ribosomes run off mRNAs during stress-induced silencing of gene expression and dissolve as the cell adapts or recovers from the stress. SGs, lacking a limiting membrane, are composed by small ribosomal subunits, early translation initiation factors eIF4E, eIF3, eIF4A, eIF4G and RNA-binding proteins that regulate mRNA structure and function (such as PABP1, Staufen, TIA-1, TIAR, HuR). In addition to these core components SGs contain other proteins that vary with cell type and with the nature and duration of the stress involved. FRAP analysis revealed that many SG-associated RNA-binding proteins rapidly shuttle in and out of SGs, supporting the notion that SGs are centers that sort, remodel, and export specific mRNA transcripts for reinitiation, decay or storage activities (Kedersha et al., 2002, 2005).

As schematized in Figure 2, in stressed cells mRNAs are thus in a dynamic equilibrium between polysomes and SGs, because disruption of polysomes promotes SGs formation, whereas polysome stabilization prevents SG assembly (Anderson and Kedersha, 2002). However, mRNA composition of SGs is specific, because they contain transcripts encoding housekeeping effectors but exclude those encoding stress-induced effectors such as heat shock proteins or repair enzymes (Anderson and Kedersha, 2009).

Among mechanisms that target RNA components of the translational machinery is notable the stress-induced cleavage of tRNAs, by ribonucleases that are normally secreted or sequestered. Cleavage of tRNAs, that occurs preferentially within the anti-codon loop, is not limited to specific tRNAs and in most cases full-lenght tRNAs levels do not decline significantly. It has been reported during a variety of stress responses in eukaryotic cells that cleavage of tRNAs is performed by specific ribonucleases evolutionary conserved in all eukaryotic organisms (Thompson and Parker, 2009).

Ribonucleases (RNases) are ancient enzymes that catalyze the degradation of RNA into smaller fragments and regulate various aspects of RNA metabolism. Housekeeping RNases play key roles in the maturation, quality control and turnover of cellular RNA, other RNases, named stress-induced RNases, are instead activated in response to stresses.

Under growth conditions, stress-induced RNases are inactivated by several mechanisms including: (i) physical compartmentalization within membrane-bound organelles such as vacuoles or nuclei, (ii) secretion into the extracellular environment, (iii) binding to RNase inhibitor. Upon stress, these enzymes are activated into the cytoplasm and cleave different RNA

substrates that can profoundly affect cellular physiology (Ivanov and Anderson, 2011). RNases activation is an intriguing new aspect of cellular stress responses, with a potential impact on apoptosis, cancer and disease progression.

Among the RNases, particularly relevant is human RNase 5 or human angiogenin (ANG), a member of the Vertebrate RNase Superfamily with different physiological functions and also involved in stress response mediated by tRNA cleavage.

1.2 The human angiogenin (ANG)

Human angiogenin (ANG) is a cationic single-chain protein with a molecular weight of about 14 kDa, secreted into the extracellular environment, known to stimulate formation of new blood vessels and cell growth. It was originally identified as a tumor angiogenic molecule from the conditioned medium of HT-29 human colon adenocarcinoma cells (Fett et al., 1985).

ANG has the consensus sequence C-K-x-x-N-T-F, shared by all members of the Superfamily, six cysteine residues involved in the formation of three disulfide bridges and a catalytic site, containing two histidines and one lysine, conserved in all vertebrates (Figure 1.3). Although its ribonucleolytic activity is about 10^6 orders lower than that of RNase A, the Superfamily prototype, it is essential for angiogenesis and a few other functions. Chemical modifications or site-directed mutagenesis on catalytic residues, turn off both the ribonucleolytic and the angiogenic activity (Shapiro and Vallee, 1987).

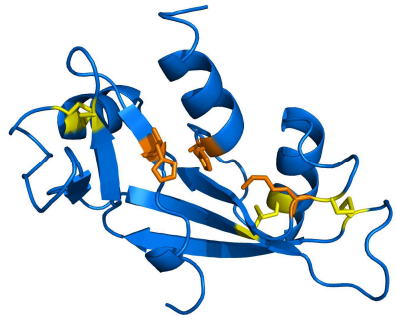

Figure 1.3 3D structure of human angiogenin. (PDB entry: 1ANG) The three disulfide bonds are shown in yellow and the the catalytic triad in orange.

ANG has been shown to undergo nuclear translocation mediated by a nuclear localization sequence (NLS) consisting of ^{30}MRRRG^{34} in proliferating endothelial (Moroianu and Riordan, 1994), cancer (Tsuji et al., 2005) and neuronal (Thiyagarajan et al., 2012) cells. Nuclear translocation of ANG occurs after receptor-mediated endocytosis, independently of microtubules and lysosomes. Upon entering in the nucleus, ANG accumulates especially in nucleoli where it stimulates rRNA transcription (Xu et al., 2002) by binding to the promoter region of ribosomal DNA (Xu et al., 2003) promoting cell growth and proliferation (Figure 1.4).

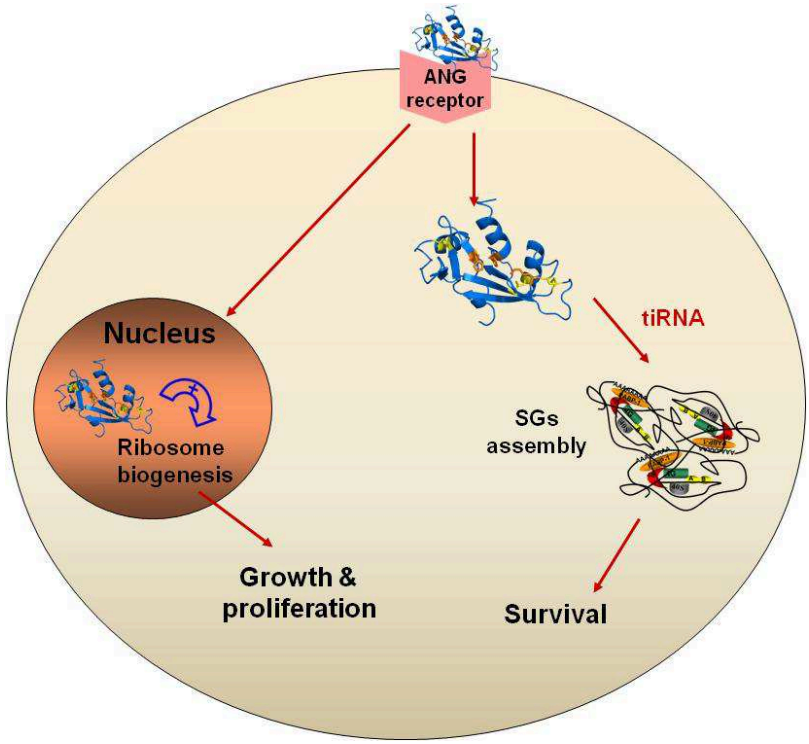

Figure 1.4 Current understanding of mechanisms of ANG (adaptation from Li, S. And Hu, G. F., 2010)

ANG-stimulated rRNA transcription is a general requirement for angiogenesis: silencing ANG expression in endothelial cells inhibits cell proliferation induced by other angiogenic factors as aFGF, bFGF, VEGF and EGF (Kishimoto et al., 2005). ANG nucleolar translocation also plays an important role for cancer cells where ANG stimulates both tumor angiogenesis and cancer cell proliferation (Tsuji et al., 2005) promoting thereby cancer progression. ANG expression is clearly up-regulated in various types of human cancers, particularly in prostate cancer. Indeed, knocking down ANG expression in PC-3 human prostate cancer cells decreases rRNA transcription, ribosome biogenesis, cell proliferation, and tumorigenicity. Furthermore gene encoding ANG is the most significantly up-regulated gene in AKT-driven prostate intraepithelial neoplasia (PIN) in mice. Silencing ANG expression by intraprostate injection of lentivirus-mediated ANG-specific small interfering RNA prevents AKT-induced PIN formation. Knocking down ANG did not affect AKT activity while it suppresses rRNA transcription thereby inhibiting cell growth and proliferation and preventing PIN formation (Ibaragi et al., 2009). Thus, ANG is an attractive target for cancer therapy and ANG inhibitors are perceived to have the benefit combining both anti-angiogenesis therapy and chemotherapy (Li et al., 2011).

The biological function of ANG has been recently extended to maintenance of normal physiological function of motor neurons, preventing neurodegeneration (Li and Hu, 2010). In contrast to being up-regulated in various cancers, ANG has been shown to be down-regulated in neurodegenerative diseases including amyotrophic lateral sclerosis (ALS) (McLaughlin et al., 2010), Parkinson's disease (PD) (Steidinger et al., 2011) and Alzheimer's disease (Kim and Kim, 2012). More importantly, loss-of-function mutations have been found in patients with ALS and PD. ANG mutations are associated with a functional loss of the angiogenic activity due to a failure in ribonucleolytic activity, nuclear translocation, or both. ANG plays a role in neuron survival and its deficiency is a serious risk factor (Li and Hu, 2010). Wild type ANG has been shown to reduce neuronal death in *in vitro* models of ALS and PD, and knockdown of ANG expression by siRNA promotes cell death (Steidinger et al., 2011). In contrast, mutant angiogenin inhibits neurite extension and promotes hypoxia-induced cell death in motoneurons (Sebastià *et al.* 2009). *In vivo*, systemic treatment with wild type ANG increases motoneuron survival and delays motoneurones dysfunction. This neuroprotective effect appears to be mediated through inhibition of apoptosis via the PI3K-AKT signaling pathway, as inhibition of

PI3K-AKT pathway disrupts ANG neuroprotection *in vitro* (Kieran et al., 2008).

The discovery of ANG's neuron survival activity is coincident with the recent finding that ANG mediates the production of tRNA-derived stress-induced RNA (tiRNA) (Yamasaki et al., 2009; Emara et al., 2010). It has been shown that tiRNAs suppress global protein translation of both capped and uncapped mRNAs. However, tiRNAs did not inhibit IRES-mediated cap-independent translation (Ivanov et al., 2011), a mechanism often used by anti-apoptosis and pro-survival genes to escape stress-activated global translation attenuation programs (Baird et al., 2006). Therefore, tiRNAs reprogram protein translation in response to stress thereby promoting cell survival (Thompson et al., 2008).

Cleavage of tRNA occurs preferentially in the anticodon loop with subsequent production of 5' and 3' fragments with length of ~30 and ~40 nucleotide, named 5' and 3' tiRNAs, respectively (Yamasaki et al., 2009). ANG cleaves only a minor (less than 10%) fraction of mature tRNAs without preferential cleavage of individual tRNA species or their isoforms. It should be noted that the RNase activity of ANG is necessary for stress-induced tiRNAs production and its knockdown inhibits tiRNAs production. Importantly, transfection of only purified 5' tiRNAs inhibits protein synthesis (Yamasaki et al., 2009).

Moreover, transfection of 5' tiRNAs has been shown also promote the assembly of SGs by eIF2α phosphorilation-independent pathway. ANG has been found enhance the formation of SG when stressed cells are treated with recombinant ANG (Emara et al., 2010). Altogether, these data support hypothesis that ANG and tiRNAs are components of an alternative stress response pattern that acts via formation of SGs and independently of global eIF2α-phosphorilation-dependent translation control.

In the cell, one of key mechanisms involved in the control ANG activities could be represented by its strong susceptibility to the interaction with the human RNase inhibitor (RNH1).

1.3 The human RNase inhibitor (RNH1)

Human RNase inhibitor (RNH1) is an ubiquitous, evolutionary conserved 50 kDa protein that avidly binds most monomeric RNases from the Vertebrate RNases Superfamily, thereby neutralizing their RNase activity (Hofsteenge, 1997). In particular the ANG/RNH1 complex is among the strongest known protein-protein interactions, for which the Kd is femtomolar (Lee et al., 1989). C-terminal end residues directly contact the residues of the

catalytic site of the RNase through electrostatic interactions and hydrogen bonds (Shapiro et al., 2000) (Figure 1.5).

Structure of RNH1 is characterized by 16 α-helices, facing outwards, and 17 segments β-parallel, facing inward, that alternate along the skeleton and form a horseshoe-shaped structure. RNH1 has a high content of leucine residues (15 leucine-rich repeats LRRs) and cysteines (32 residues).

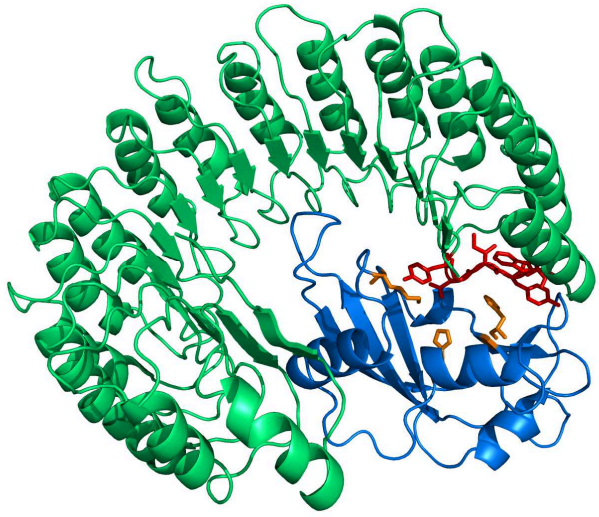

Figure 1.5 3D structure of ANG/RNH1complex. (PDB entry: 1A4Y) C-terminal end residues (in red) directly contact the residues of the catalytic site of ANG (in yellow).

This protein requires a reducing environment to preserve its inhibitory activity. In non-reducing conditions the thiol groups of cysteines are involved in the formation of disulfide bridges preventing binding to RNases, and greatly increasing its susceptibility to proteasomal degradation pathway. It has been demonstrated that the oxidation of thiol groups in RNH1, induced by a general oxidant, as H_2O_2, or with a thiol specific oxidant, as diamide, cause the loss of RNH1 activity (Blázquez et al., 1996). Importantly, in ANG/RNH1 complex the cysteine residues of RNH1 are reduced and the disulfide bridges of ANG remain unaffected (Dickson et al., 2005). LRRs consisting of approximately 22–28 amino acids are structural motifs present in numerous proteins, with different functions, usually involved in the formation of protein-protein interactions (Bella et al., 2008).

With regard to the physiological role of RNH1 several hypotheses have been advanced, none of which fully accepted (Figure 6).

According to one of the theories, the function of this protein would be to protect the cellular RNA from degradation by extracellular RNases (Dickson et al., 2005). RNH1-resistant RNases, such as bovine seminal RNase or onconase, are cytotoxic (D'Alessio and Riordan, 1997) and display a more powerful cytotoxic effect on cells deprived of RNH1. Non-cytotoxic RNases, strongly inhibited by RNH1, become cytotoxic when they are engineered into relatively RNH1-resistant RNases (Leland et al., 1998). Notwithstanding, the knockdown of RNH1 in HeLa cells does not allow to a non-cytotoxic RNase, such as RNase A or human pancreatic RNase, to become cytotoxic (Monti and D'Alessio, 2004).

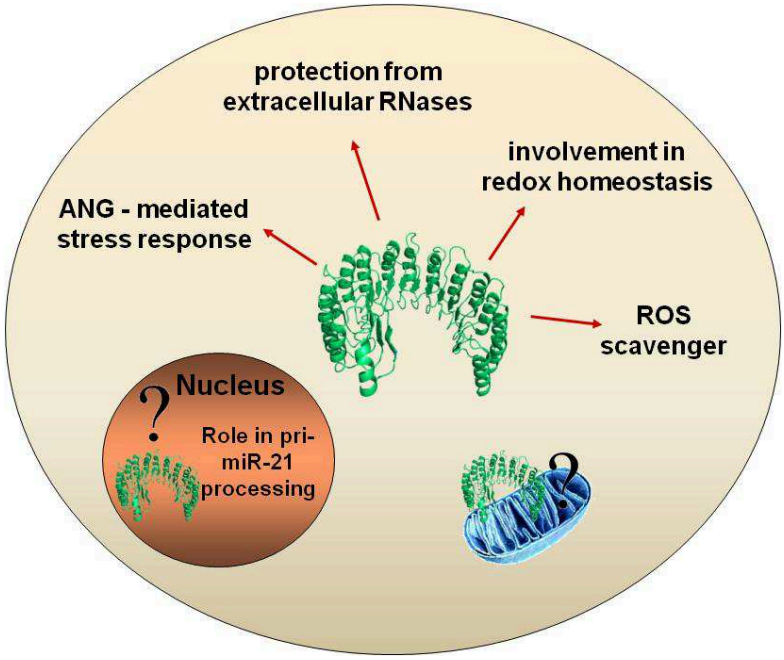

Figure 1.6 Hypothetical cellular mechanisms of RNH1

A more intriguing hypothesis regards the involvement of RNH1 in maintaining the redox homeostasis of the cell, through its high content in cysteines (Blázquez et al., 1996).

It has been also reported that overexpression of RNH1 renders cells more resistant to the oxidant action of H_2O_2 (Monti et al., 2007) and that RNH1 has a scavenging activity on reactive oxygen species (ROS) (Wang and Li, 2006). It has pointed out that RNH1, purified by cow placenta, displays *in vitro* radical scavenging activities dose-dependently toward different ROS, including superoxide anion (O_2^-), hydroxyl radical (OH•) and lipid derived radicals (R•).

Recently data obtained at the subcellular level have shown that RNH1 is present not only in the cytoplasm but also in mitochondria and nucleus, supporting the hypothesis of a key physiological role of RNH1 in redox homeostasis (Furia et al., 2011). Other results demonstrated the association of RNH1 with proteins of the mitochondrial inner membrane and matrix, both featured by high level ROS production. So, although, there is not a complete understanding of the cytoplasmic functions of this protein, new nuclear and mitochondrial roles have begun to emerge.

A new aspect of RNH1 in the regulation of gene expression has emerged, giving to RNH1 a role regulatory of microRNA (miRNA) biogenesis in nucleus (Kim et al., 2011). Nuclear RNH1 facilitates pri-miR-21 processing, through the direct interaction with the Drosha complex. It has been shown that miR-21 is overexpressed in almost all types of cancer, playing key oncogenic roles in cancer initiation and progression. Drosha complex has a role in the biogenesis of miRNAs cleaving the pri-miRNAs into shorter pre-miRNAs in the nucleus. PTEN, a tumor suppressor frequently mutated in many cancers, inhibits miR-21 expression. It has been evidenced that PTEN interacts with RNH1, blocking the interaction with Drosha, thereby reducing pri-miR-21 processing. However, it remains to be determined whether RNH1 regulates the processing of other miRNAs and whether the regulation is sequence specific.

It has been recently described a further role of RNH1 in ANG-mediated response to stress. It has been observed that RNH1 regulates ANG-mediated tiRNAs production and so repression of cellular translation. Knockdown of RNH1 enhances tiRNAs production in cells subjected to oxidative stress, leading to translational arrest (Yamasaki et al., 2009). Moreover, RNH1 overexpression inhibits ANG-mediated assembly of SGs in U2OS cells exposed to oxidative stress indicating that RNH1 abrogates the effects of ANG on stimulating SGs assembly (Emara et al., 2010).

1.4 Aims

Cellular stress plays an important role in the onset of cancer and neurodegenerative diseases where processes of autophagy and apoptosis are induced, with the accumulation of toxic substances and cell damaging. As previously described ANG has an active role in these pathologies, as well as in stress response. An intriguing question yet to be answered is how ANG activity is regulated to properly stimulate, under growth and stress conditions, rRNA transcription and tiRNAs production, respectively. To this respect the action of RNH1 could play a prominent role in regulation of ANG roles under different conditions. Furthermore, considering that RNH1 could be directly involved in the stress response, as ROS scavenger, it appeared extremely intriguing to study the intracellular behaviour of both proteins under stress, by alternative experimental approaches.

In the present work most cellular stress is represented by oxidative stress induced by sodium arsenite (SA) in HeLa cells. The oxidative stress is an underlying mechanism of many disease processes. Especially, SA is known for its genotoxic effects caused by a still not known mechanism of ROS generation (Jomova et al., 2002). Trivalent inorganic arsenic inhibits numerous cellular enzymes, through binding to their sulfydryl group. One of the consequences is the inhibition of glutathione production, which normally protects cells against oxidative damage (Miller et al., 2002). Moreover, exposure to the arsenite anion contributes to human pathogenesis (Abernathy et al., 1999), resulting in skin disease, cancer, peripheral neuropathy and cardiovascular disease, in which it can be assumed that cell proliferating mediated by ANG plays a pivot role.

ANG is known to play two different physiological roles in growth and stress conditions in two different cell compartments; thus, the first goal was to verify whether a change in subcellular localization of ANG and RNH1 occurred in stress response.

Furthermore, since both proteins are involved in RNA metabolism, a second goal was to verify a possible colocalization of RNH1 and ANG with SGs, a hallmark of stress response, and their engagement in the pathway of SGs assembly.

Then, it was interesting to analyze whether RNH1 could affect the intracellular behavior of ANG, under different growth conditions.

Understanding and elucidate ANG and RNH1 function and mechanism in stress response could be significant to exploit both proteins as novel target for cancer and neurodegenerative disease therapy.

2. Materials and Methods

2.1 Cell cultures and treatments

All cell lines were grown at 37°C in 5% CO_2 incubator. HeLa cells were maintained in Dulbecco's modified Eagle medium (DMEM) supplemented with 10% fetal bovine serum (FBS), 1mM L-glutamine, 1% v/v penicillin/streptomycin solution (100 Unit/ml) (Sigma-Aldrich, Milano, Italy). LNCaP cells were maintained in RPMI 1640 supplemented with 10% FBS. H9c2 cells were grown in DMEM supplemented with 10% fetal bovine serum (FBS), 2mM L-glutamine, 1% v/v penicillin/streptomycin solution (100 Unit/ml) and 1mM sodium pyruvate.

Oxidative stress was induced by sodium arsenite (SA) (Sigma Aldrich) used at 0.5 mM for 1 hour or otherwise indicated, prepared in stock aqueous solutions and added to conditioned medium. In the stress-recovery experiments, medium containing SA was removed and cells were washed 3 times with medium and cultured in growth medium at 37°C for 3 hours. To induce ER stress, cells were treated with 5 μg/ ml tunicamycin for 24 hours. Heat shock was performed by exposing cells at 42°C in a CO_2 incubator for 30 min.

2.2 Cellular extracts

Cytosolic extracts were prepared as follows: cells were scraped in ice cold phosphate buffered saline (PBS) and lysed in 10 mM HEPES buffer at pH 7.4 containing 5mM $MgCl_2$, 300 mM KCl, 0.5% NP-40, 1mM DTT and protease inhibitors 1X (Roche, Milano, Italy) for 30 minutes. After centrifugation at 14,000 rpm for 30 min at 4°C, supernatants were collected and analyzed. Protein concentration was measured by the Bradford method (Sigma Aldrich) using bovine serum albumin (BSA) as molecular weight standard and subsequently analyzed by Western blot analysis.

Nuclear extracts were prepared by centrifugation on a 30% sucrose cushion to protect nuclei and strip away cytoplasmic contaminants (Kihlmark and Hallberg, 1998). Briefly, cells were scraped in ice cold 10 mM HEPES at pH 8.0 containing 1 mM EDTA, 60 mM KCl, 0.2% NP-40, 1mM Na_3VO_4, 1 mM DTT and protease inhibitors 1X (Roche). Nuclei were collected after centrifugation at 2,500 rpm for 5 min at 4°C, washed in the same buffer excluding the detergent and layered on a sucrose cushion previously prepared in the same buffer. After a centrifugation at 6,000 rpm for 10 minutes at 4 °C, the sedimented nuclei were resuspended in 250 mM Tris-HCl buffer at pH 7.8 containing 60 mM KCl, 1 mM Na_3VO_4, 1 mM DTT and protease inhibitors. Lysis of nuclei was performed by freezing in dry ice followed by thawing at 37°C (three times). After centrifugation at 9,500 rpm for 15 min 4°C, supernatants were collected and analyzed.

Protein concentration of cellular extracts was measured by Bradford method (Sigma Aldrich) and subsequently analyzed by Western blot analysis.

2.3 Immunofluorescence and confocal microscopy

Cells were seeded onto coverslips (20.000 cells in 400µl of DMEM for each coverslip) and grown for 48 hours. Cells were fixed in methanol at -20°C for 10 min, rinsed in PBS, and incubated in blocking buffer (5% BSA in PBS). The fixed cells were then incubated with ANG mAb 26-2F (5µg/ml) or affinity-purified ANG pAb R113 (2µg/ml), affinity-purified RNH1 pAb R127 (2µg/ml) (all of them were a kind gift from Dr Hu G. F., Tufts Medical Center, Boston, USA), PABP mAb (Sigma Aldrich) and RPS3 mAb (Sigma Aldrich), diluted in blocking buffer. After washing in PBS, the secondary antibodies used were Alexa488 conjugated goat anti-rabbit or Cy3 conjugated goat anti-mouse $F(ab')_2$ (1:1000 dilution) (Jackson ImmunoResearch Laboratories, United of Kingdom). For nuclear staining the cells were then incubated with DAPI (Molecular Probes, Invitrogen, Italy) 0.1 µg/ml in PBS for 10 min at room temperature. After washing, coverslips were mounted in PBS containing 50% glycerol.

Confocal microscopy was performed with a confocal laser scanner microscope SP5 Leica. The lambda of the argon ion laser and He-Ne laser was set at 488 nm and 546 nm, respectively. Fluorescence emission was revealed by band pass 500–530 and 560–650, respectively, for Alexa488 and Alexa546. Double staining IF images were acquired separately in the green and red channels and then saved in Tiff format at a resolution of 512x512 pixels.

2.4 Gel filtration Chromatography

Size exclusion chromatography of cytoplasmic extracts from $6x10^6$ HeLa cells, diluted in PBS, was carried out with the AKTA Purifier System (Amersham Biosciences, Milano, Italy) on a Superdex G-200 (30 cm x 1 cm, 25 ml) previously equilibrated in PBS containing 100mM NaCl. The eluate was monitored at 260 and 280 nm, collected in 0.25 ml fractions and analysed for ANG and RNH1 contents by Western blot.

2.5 Sucrose gradient ultracentrifugation

HeLa cells were scraped in ice cold PBS, pelleted and lysed in ice cold 10 mM HEPES buffer at pH 7.4 containing 5mM $MgCl_2$, 300 mM KCl, 0.5% NP-40, 5mM DTT and protease inhibitors for 30 minutes. Following centrifugation at 14,000 rpm for 30 min at 4°C supernatants were layered onto ice cold 60-15% sucrose gradients (10 mM HEPES, pH 7.4, 5mM Mg_2Cl and 300 mM KCl).

After centrifugation at 38,000 rpm overnight at 4°C in a Beckman SW 41 rotor, the gradient fractions 0.5 ml were collected from the bottom of the tubes using a peristaltic pump (Pharmacia). The polysomal profile was monitored by UV absorbance at 254 nm. Proteins, from selected fractions, extracted by precipitation in methanol-chloroform (Wessel and Flugge, 1984), were analyzed for ANG, RNH1, PABP and RPS3 by Western blot.

2.6 RNase activity assay

Representative fractions obtained by sucrose gradient ultracentrifugation (fractions 1-3-5-7) were analysed. Samples were incubated in 40 mM HEPES at pH 7.0 containing 250 mM NaCl, 2 mM EDTA and 5 mM DTT for 10 minutes at 37 °C. The assay mixture, containing yeast tRNA (2µg) was then incubated for 30 minutes at 37 °C, subsequently loaded on an 1.5% agarose gel and stained with ethidium bromide.

2.7 Fractionation of Lysates with NP-40 detergent

Untreated or arsenite treated HeLa cells were washed in ice-cold PBS and lysed in ice-cold extraction buffer containing 20 mM Tris, pH 7.4, 50 mM KCl, 0.5% NP-40 and protease inhibitors 1X. The cells were scraped from the dishes, harvested in the buffer and rotated in the cold room for 30 min. The cell lysates were then sonicated for 2x2 min in a water-bath, prior to centrifugation at 14,000*g* for 25 min at 4°C. The supernatants (soluble fraction) were removed and the NP-40-resistant pellets (insoluble fraction) were resuspended in lysis buffer containing 2% SDS, heated to 95°C for 5 min, sonicated, and analyzed by Western blot.

2.8 FRET analysis

FRET analysis was carried out on HeLa cells fixed, by acceptor photo-bleaching method. The cells were fixed with 4% paraformaldehyde, and permeabilized with 0.1% Triton X-100 following quenching with 50mM NH_4Cl. ANG mAb 26-2F (5µg/ml) and affinity-purified RNH1 pAb R127 (2µg/ml) were used in the blocking solution (5% BSA in PBS). Alexa488 conjugated goat anti-mouse or Cy3 conjugated goat anti-rabbit $F(ab')_2$ (1:1000 dilution) (Jackson ImmunoResearch Laboratories) were used to detect ANG (donor) and RNH1 (acceptor) respectively.

The donor (Alexa488) was excited at 488 nm and detected at 500-530 nm. The acceptor (Cy3) bleaching was performed at 592 nm for 5 sec. FRET was measured by the increase of donor fluorescence intensity after Cy3 photo-bleaching. Alexa-488 fluorescence intensity in the selected ROI was recorded before (I_{DA}) and after Cy3 photo-bleaching (I_D). Measurements were performed on regions of interest (ROIs) in cytoplasm under growth conditions (n=10) and in SGs under stress conditions (n=7). To ensure reproducibility and reliability of Alexa488 fluorescence measurements, Cy3 was photo-bleached to <10% of its initial fluorescence. Efficiency of FRET was calculated as $E = (I_{DA} - I_D)/I_D$ where I_D and I_{DA} are fluorescence intensities before and after photo-bleaching.

2.9 Co-Immunoprecipitation

HeLa cells were detached by trypsin-EDTA and resuspended in 10 mM HEPES, pH 8.0, containing 10 mM KCl, 1.5 mM $MgCl_2$, 0.5 mM DTT, and 1x proteinase inhibitors cocktail and incubated on ice for 10 min. The cells were lysed by adding NP-40 (10%) to a final concentration of 0.1%. Cytoplasmic fraction was obtained by centrifugation at 1,000 x g for 5 min. The pellet was dissolved in RIPA buffer (25 mMTris-HCl, pH 7.6, 150 mMNaCl, 1% NP-40, 1% sodium deoxycholate, 1x proteinase inhibitors cocktail) and was designated as the nuclear fraction. The purity of the cytoplasmic and nuclear fractions was examined by Western blot analyses of β-tubulin and Proliferating Cell Nuclear Antigen (PCNA), respectively. For co-IP experiments, the cytoplasmic and nuclear fractions from $4x10^6$ cells were diluted in 1 ml of 10 mM HEPES containing 0.1% NP-40. A fraction of 50 µl was taken and used as input control. The remaining materials were divided into 3 equal fractions, incubated with 5 µg of non-immune mouse IgG, ANG mAb 26-2F, or affinity-purified RNH1 pAb R127 at 4°C. Five µl from each sample was taken for β-tubulin and PCNA analysis. The remaining solution was mixed with 50 µl of 50% Protein A/G-Sepharose by rotating at 4°C for 2 h. The mixture was centrifuged, washed, and analysed by Western blot for ANG and RNH1 with R113 and R127, respectively.

2.10 RNH1 knockdown

A set of human RNH1 specific shRNA cloned in pLKO.1 lentiviral vector was purchased from Open Biosystems. Five specific shRNA constructs were chosen per gene to ensure adequate coverage of the target gene RNH1. Lentiviral particles were packaged in HEK293T cells (60% confluence) co-transfected with shRNA/pLKO.1 (5.8 µg), envelope plasmid pMD2.G (1.8 µg), and packaging plasmid psPAX (4.4 µg).

After 48 hours co-transfection, recombinant lentiviral particles released into the supernatant were collected. Particularly, the cells and debris were eliminated by centrifugation at 1100 rpm for 5 minutes and subsequent filtration (0.45 μm, Millipore). Lentivirus-containing supernatants were concentrated with Lenti-X Concentrator (Clontech) and the mixtures were incubated at 4°C overnight. Following centrifugation at 1500 x g for 45 min at 4°C, lentivirus-containing pellets were resuspended in PBS (1/10 of the original volume). HeLa cells were infected with lentivirus in the presence of 10 μg/ml polybrene for 48 h. Puromycin-resistant (1.5 μg/ml) cells were selected and the level of RNH1 was examined by Western blot analysis with pAb R127.

2.11 EB/AO staining of apoptotic cells

HeLa cells transfected for RNH1 knockdown (scramble control and sh35 transfectants) were seeded in six-well dishes (200.000 cells in 2 ml of DMEM) and grown for 48 hours. Apoptotic cells were identified by EB/AO staining (Ribble et al., 2005). Cells before or after SA treatment (1 mM for 1 h) were trypsinized, pelleted, and washed with ice cold PBS 1X. The cells were re-suspended in 100μl of ice cold PBS and mixed with 5μl of the EB/AO dye mixture (100 μg/ml each of AO and EB in PBS 1X) at 37^{o}C for 20 min. Stained cells were placed on a microscope slide and covered with cover slips. Images were taken at 200 X magnification. Both apoptotic (red) and live (green) cells were counted in five microscopic fields, to obtain the percentage of apoptotic cells.

2.12 Western blotting

Proteins from cytoplamic and nuclear extracts, chromatographic fractions or sucrose gradient fractions were resuspended in Laemmli sample buffer (in the presence of 2% SDS and 0.4M β-mercaptoethanol), separated by SDS-PAGE, and electrotransferred to Immobilon-PVDF membranes (Millipore, Bedford, MA, USA). PVDF membranes were incubated in blocking solutions (PBS containing 0.1% Tween-20 and 5% bovine serum albumin) at room temperature for 1 h and incubated with primary antibodies overnight at 4°C.

Primary antibodies were diluted in blocking solution as follows: affinity-purified ANG pAb R113 (1 μg/ml), affinity-purified RNH1 pAb R127 (1 μg/ml), PABP mAb (Sigma Aldrich, 0.5 μg/ml) RPS3 mAb (Sigma Aldrich, 0.5 μg/ml). After washing, the membranes were incubated with horseradish peroxidase conjugated goat anti-mouse or anti-rabbit IgG (1:10000) (Fc specific, Roche, Italy).

Detection by intensified chemiluminescence was performed according to the manufacturer's instructions (Super Signal®West-Pico Chemiluminescent Substrate, Pierce, Rockford, IL), using a Phosphorimager (Biorad, Italy).

3. Results

3.1 Differential subcellular localization of ANG and RNH1 under growth and stress conditions

ANG and RNH1 are located both into the cytoplasm and nucleus of human cells (Lee and Vallee, 1993; Moroianu and Riordan, 1994b; Furia et al., 2011). The biological activity of ANG is correlated to cell growth and proliferation through rRNA transcription (Gao and Xu, 2008). In nuclear fraction ANG would be free, especially in nucleoli, to induce ribosomes biogenesis, while in the cytoplasm, to avoid random RNA degradation, it is expected that ANG is tightly bound to RNH1, due to their high binding affinity. Moreover, the biological activity of ANG is also correlated to stress response through tiRNAs production (Yamasaki *et al.*, 2009) promoting consequently a transient translational arrest. In this case ANG should be RNH1 free so that it can exert its ribonucleolytic activity, required to induce tRNAs cleavage. It appears conceivable to hypothesize a fine regulation of ANG subcellular localization under different growth conditions.

To determine if there was a direct link between the subcellular location of two proteins, first experimental approach has focused to value protein levels of ANG and RNH1 in cytoplasm and nucleus of HeLa cells cultured under different growth conditions. Western blot analysis (Figure 3.1, panel A) has revealed that in the nuclear fraction, ANG levels decrease under stress conditions, induced by sodium arsenite (SA) (Figure 3.1, panel A, upper lanes). Into the cytoplasmic fraction, instead, an opposite pattern occurs: ANG is present at very low concentrations under growth conditions, whereas under stress conditions an increasing of protein level occurs (Figure 3.1, panel A, lower lanes). Oxidative stress causes a shift of ANG distribution from nucleus to cytoplasm: more ANG is located in the cytoplasm than in the nucleus. This different subcellular localization of ANG under growth and stress conditions reflects its role in stimulating nuclear rRNA transcription and cytoplasmic tiRNA production, in respective conditions.

The subcellular distribution pattern of RNH1 was opposite to that of ANG. In nucleus, stress involves a slight increase of RNH1 level (Figure 3.1, panel B, upper lanes). Instead, in the cytoplasmic fraction more RNH1 was identified under growth condition than in SA-induced stress conditions (Figure 3.1, panel B, lower lanes). Maybe oxidative stress induces formation of disulfide bridges on RNH1 and consequently its greater susceptibility to the degradation mediated by proteasome (Blazquez et al.,1996). Whereas nuclear RNH1 could respond to stress with improved capability to maintain redox state.

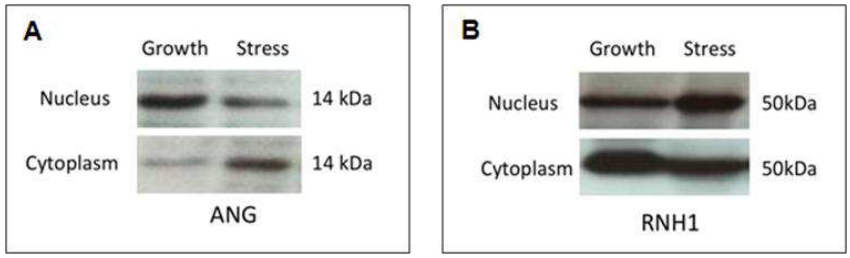

Figure 3.1 Differential subcellular localization of ANG and RNH1 by Western blot analysis in HeLa cells. ANG (panel A) and RNH1 (panel B) in nuclear (upper lanes) and cytoplasmic fractions (lower lanes). HeLa cells were cultured under growth and stress conditions (0.5 mM SA at 37^{o}C for 1h).

To substantiate and eventually identify more details of the subcellular trafficking of both proteins and their regulation under growth and stress conditions, an immunofluorescence (IF) experiment was performed.

A double immuno-staining was done to follow the localization of ANG and RNH1 into the cell, under growth and stress conditions. Consistent with Western blot results, into the cell under growth conditions, ANG was mainly detected in the nucleus, while its detection in cytoplasm was less strong (Figure 3.2A, left panel). Also, ANG was concentrated in the perinucleolar region where rRNA processing and assembling take place (Nazar, 2004) (indicated by arrows in the figure).

Under growth conditions, RNH1 was identified strongly both in the nucleus, but not in the nucleoli, and in the cytoplasm, although with a lower intensity (Fig 3.2A, second panel, nucleoli were indicated with dashed arrows). Merged images revealed small widespread yellow spots that indicated a co-localization of ANG and RNH1, but clearly not in the nucleoli (Fig 3.2A, right panel). Under growth conditions it is possible assume that at least in nucleoli, ANG is not associated with RNH1 and accordingly inhibited, so that it is able to activate rRNA transcription.

Oxidative stress induced, as well as demonstrated by Western blot analysis, a less nuclear localization of ANG (Figure 3.2B, left panel) and a higher accumulation of RNH1 in the nucleus (Figure 3.2B, second panel). Moreover, both proteins showed a staining shaped of larger spots, in the cytoplasm (indicated by arrows). From merged images (Figure 3.2B, right panel), two types of cytoplasmic spots were identified for ANG staining: those colocalized with RNH1 (indicated by arrows), and those free of RNH1 (indicated by arrowheads).

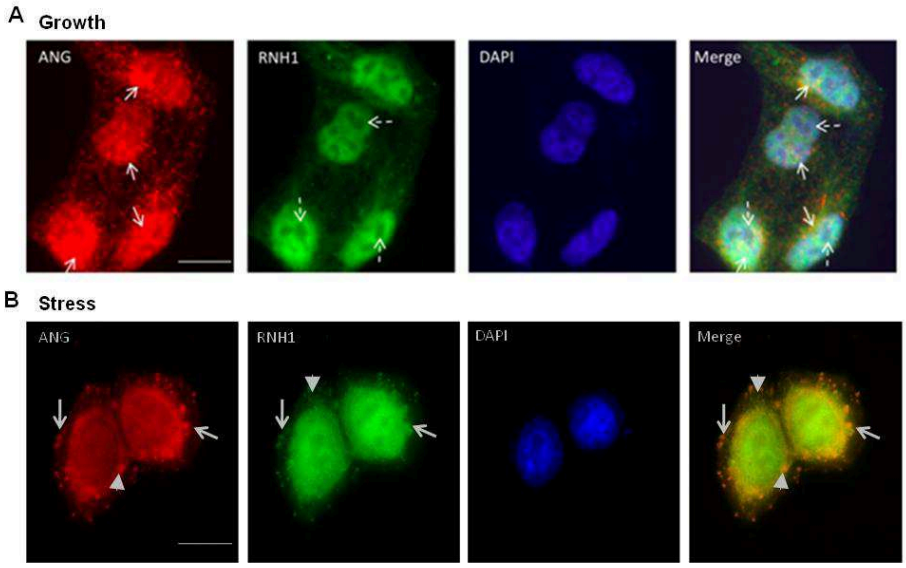

Figure 3.2 Differential subcellular localization of ANG and RNH1 by IF analysis in HeLa cells. ANG and RNH1 in HeLa cells cultured under growth (A) and SA-induced stress (B) conditions. Nuclei were stained with DAPI. Arrows indicate ANG perinucleolar signal in upper left panel, and overlapping signals of ANG and RNH1 in merge image. Dashed arrows indicate nucleoli. Scale bars, 10 μm.

So ANG and RNH1 are differently located into the cell and are oppositely regulated by stress. Under stress conditions, ANG is strongly reduced in the nucleus suggesting that ANG leaves nucleus to reduce rRNA transcription and preserve anabolic energy needed to stress-induced damage

repair promoting cell survival. On the contrary, oxidative stress leads in decrease of RNH1 level into the cytoplasm and at the same time RNH1 seems to increase in the nucleus. Under stress conditions cytosolic RNH1 is likely submitted to a partial degradation mediated by the proteasome. Less clear is the role for nuclear RNH1: it could inhibit the trace amount remaining ANG or could be more involved in stress response in maintaining the nuclear redox homeostasis through its high content in cysteines.

Similar results were obtained also with two different cell lines, LNCaP and H9c2. LNCaP are androgen-sensitive human prostate adenocarcinoma cells in which ANG overexpression plays a pivot role in their highly tumorigenic phenotype. H9c2 are embryonic rat cardiomyoblastic cells and they are currently used as model system of non-malignant and cardiac-like cells, suitable to study cellular responses to oxidative damage. IF analysis (Figure 3.3) pointed out that oxidative stress, mediated by SA, induced in both cell lines a shift of ANG from nucleus to cytoplasm and, opposite, a more RNH1 nuclear localization. It has also be noted that in both stressed cell types, ANG and RNH1 co-localized in the cytoplasm in some large spots (yellow dots in Figure 3.3) as well as detected in HeLa cells (Figure 3.2).

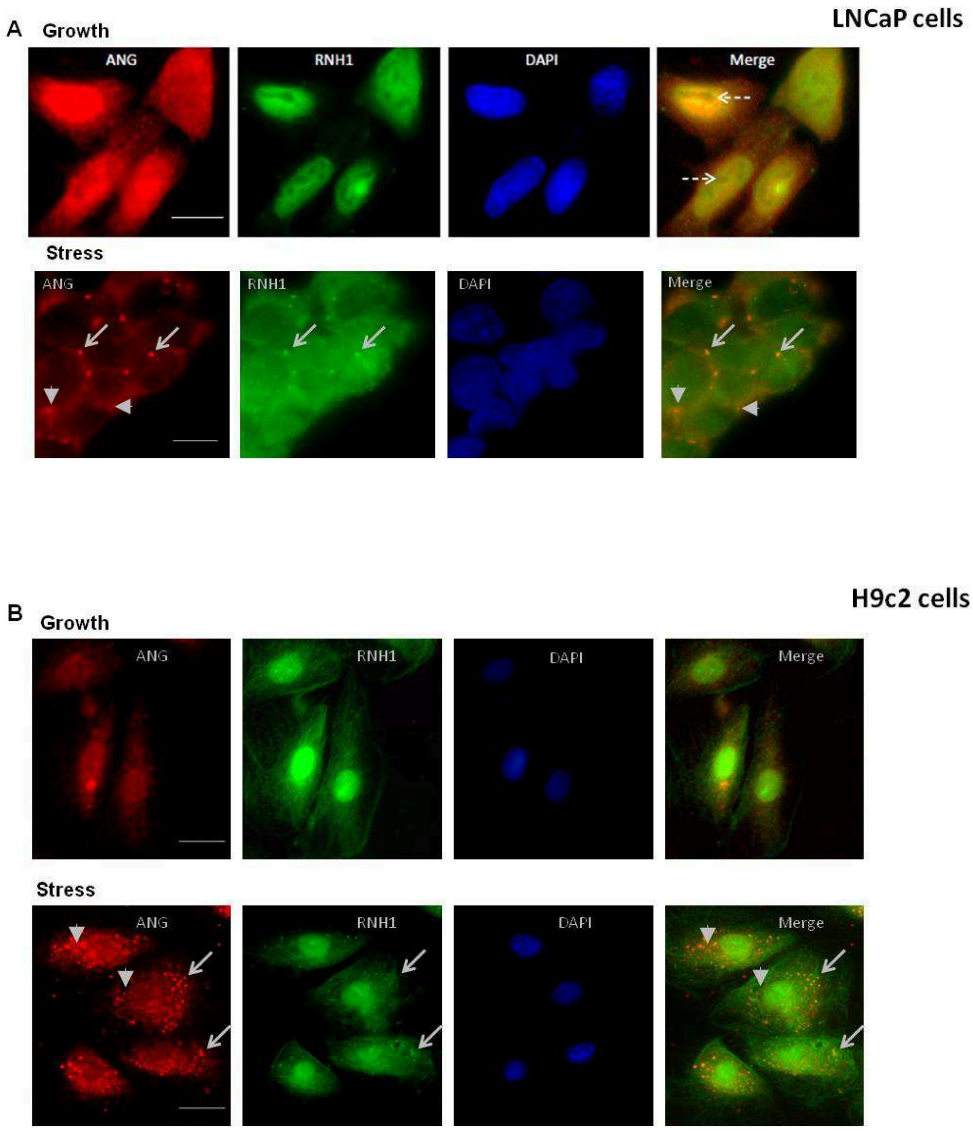

Figure 3.3 Differential subcellular localization of ANG and RNH1 by IF analysis in LNCaP and H9c2 cells. ANG and RNH1 in LNCaP (panel A) and H9c2 cells (panel B) under growth and stress conditions. Arrows indicate overlapping signals of ANG and RNH1. Arrowheads indicate ANG signals non-overlapping with RNH1. Dashed arrows indicate nucleoli. Scale bar, 20 μm.

By further tests it was proved that diamide (oxidative agent, data not shown), ER stress induced by tunicamycin and heat shock stress, determined a similar pattern of localization and trafficking of both proteins (Figure 3.4). In general it seems to be possible assert that the behaviour of ANG and RNH1 does not change according to the cell line used or type of stress induced.

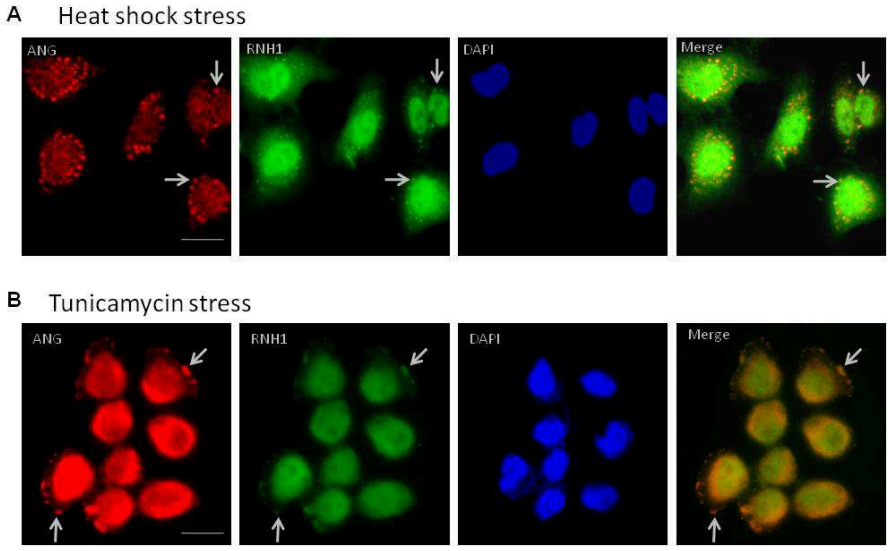

Figure 3.4 Tunicamycin and heat shock induce changes of subcellular localization of ANG and RNH1. HeLa cells were subjected to heat shock at 42°C for 30 min (A) or treated with 5 µg/ml tunicamycin (B) for 24 h. Arrows indicate overlapping signals of ANG and RNH1. Scale bar, 10 µm.

3.2 Oxidative stress induces redistribution of cytoplasmic ANG and RNH1 into supramolecular complexes

Large cytoplasmic dots of both ANG and RNH1 pointed out in stressed cells (Figures 3.2, 3.3 and 3.4) suggest that both proteins may redistribute in some cytoplasmic organelles or into some supramolecular structures. At this regard it has been carried out an experiment to verify whether in cells exposed to stress a subcellular movement of both proteins occurs to redirect both proteins on specific cytoplasmic supramolecular complexes.

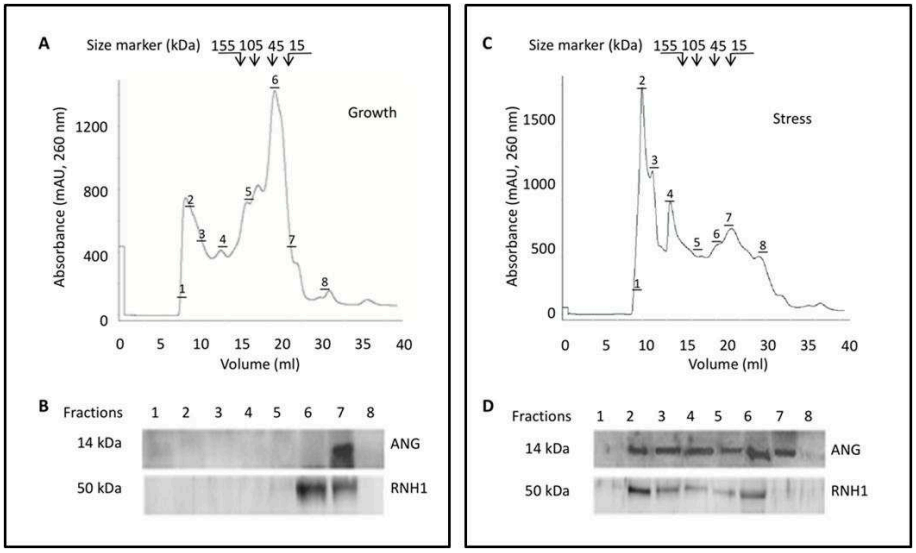

Figure 3.5 Oxidative stress induces assemble of cytosolic ANG and RNH1 into high molecular weight complexes. Gel filtration chromatography on a Superdex G-200 column of cytosolic extracts. HeLa cells were cultured under growth (A, B) and stress conditions (C, D). Stress was performed by 0.5 mM SA for 1h at 37°C. (A, C) The elution profiles recorded as milli-absorbance-units at 260 nm. The arrows indicate the elution volume of size markers (see Methods). (B, D) Selected fractions (indicated by numbers in A and C) were analyzed for ANG and RNH1 by Western blot.

Cytoplasmic extracts isolated from HeLa cells under growth and SA-induced stress conditions were resolved by gel filtration chromatography on a Superdex G-200 column. The absorbance profile obtained at 260 nm for

extracts prepared from untreated cells, was found to be strikingly different with respect to that one obtained from stressed cells (Fig 3.5A and 3.5C).

In Figure 5C it was clear that oxidative stress induced a drastic shift of the absorbance determining an increasing towards higher molecular weight fractions, suggesting the formation of high molecular weight ribonucleoprotein complexes. More intriguing was the change in elution profile of ANG and RNH1 (Figure 3.5B and 3.5D), owing to conditions change. Analyzing by Western blotting analysis representative fractions of elution profile from extracts of cells cultured in growth conditions, RNH1 and ANG were eluted, as expected, in the low-molecular-size regions of the elute. Particularly, ANG was detected only in fraction 7 (Figure 3.5B, upper lanes) and RNH1 was detected in fractions 6 and 7 (Figure 3.5B, lower lanes), suggesting that ANG and RNH1 existed as monomeric forms in the cytoplasm. Whereas under stress conditions ANG and RNH1 showed a wider distribution in the cytoplasm, detecting ANG from fractions 2 to 7 (Figure 3.5D, upper lanes) and RNH1 from fractions 2 to 6 (Figure 3.5D, lower lanes), suggesting that both proteins were eluted also in the high-molecular-size fractions. These results are in line with previous IF data in which ANG and RNH1 were localized in various large cytoplasmic foci, under stress conditions.

3.3 Stress-induced assembling of ANG and RNH1 in SGs

In order to verify whether these supramolecular complexes were SGs, IF experiments have been carried out. At this regard a monoclonal antibody specific for PABP (PolyA-binding protein) has been used as marker of SGs. As shown in Figure 6 (A and B, second panels) upon SA treatment SGs were clearly identified by PABP mAb. Double IF on SA-stressed HeLa cells with ANG pAb (R113) and PABP mAb have showed co-localization of ANG and PABP (Figure 3.6A, right panel, indicated by arrows), indicating that ANG was localized in SGs.

It is also notable that some of the ANG dots in the cytoplasm did not colocalize with PABP (Figure 3.6A, right panel, indicated by arrowheads), indicating that ANG was also present in cytoplasmic organelles that are not SGs. Double IF was carried out also with RNH1 pAb and PABP mAb. RNH1 was present in both SGs and non-SG organelles (Figure 3.6B, right panel).

These results demonstrate that oxidative stress induce localization of both ANG and RNH1 in SGs. Importantly, not in all the granules is possible to find the same double staining of both proteins. All the PABP-containing SGs were overlapped with ANG, but at the same time there was not a complete overlap between RNH1 and PABP-containing SGs (Figure 3.6A and 3.6B, right panels, indicated by dashedarrows). These data suggested that ANG and RNH1 were co-localized only in some but not in all SGs.

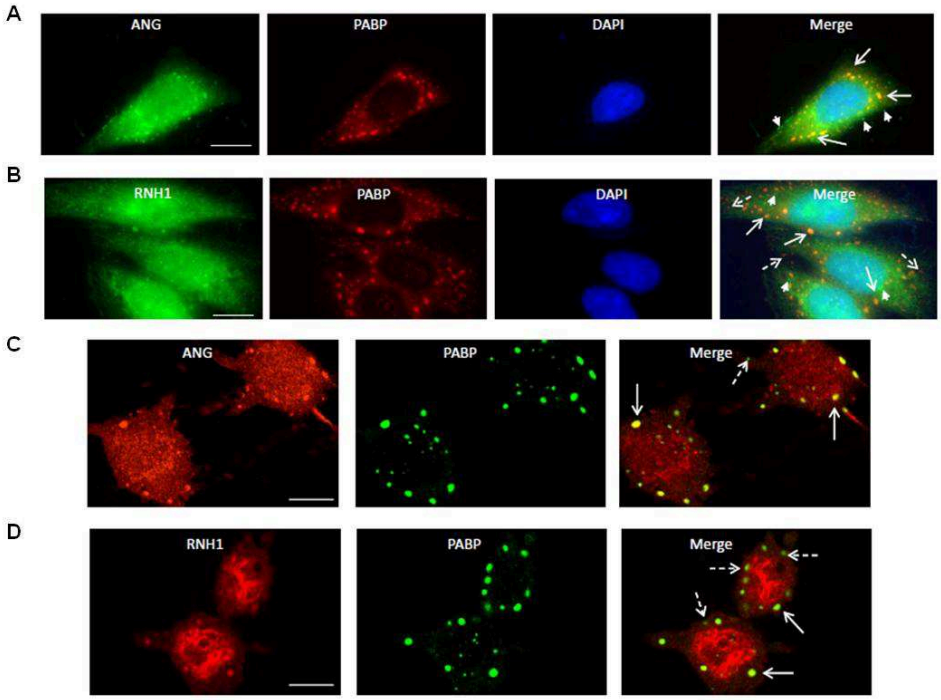

Figure 3.6 Detection of ANG and RNH1 in SGs by IF. HeLa cells were cultured in stress conditions with 0.5 mM SA for 1 h. (A) Double IF for ANG and PABP. Arrows indicate ANG signals in SGs. Arrow heads indicate staining of ANG in cytoplasmic organelles that are not SGs. (B) Double IF for RNH1 and PABP. Arrows and arrowheads indicate RNH1 signals in SGs and non-SGs cytoplasmic organelles. Scale bars, 10 µm.
(C, D) Confocal images of ANG and PABP (C) and RNH1 and PABP (D) double IF staining. Arrows indicate SGs that were stained both by ANG and PABP (C) or byRNH1 and PABP (D). Dashed arrows indicate SGs that contain only PABP. Scale bar, 10 µm.

Confocal microscopy confirmed these data: ANG was in all the SGs but RNH1 was only in some of the them (Figure 3.6C and 3.6D): through a statistic count of SGs there was a 97% ANG coverage, meanwhile RNH1 occupancy was represented for 33%. Thus a fraction of cytoplasmic ANG under stress conditions is RNH1 free, in line to arresting of protein synthesis through tRNAs cleavage and consistent with previous data obtained. Very similar results were obtained in LNCaP and H9c2 cells and in HeLa cells exposed to alternative stress conditions (data not shown) suggesting that localization of ANG and RNH1 in SGs and their different occupancy extent are a general phenomenon.

In order to confirm the recruitment of ANG and RNH1 to SGs, a biochemical approach was performed. It has noted that upon fractionating of extracts from stressed cells, SGs components can be located in a detergent-insoluble cell fraction (Lindsay and McCaffrey, 2011). HeLa cells under growth and SA-induced oxidative stress conditions were sonicated in NP-40 containing buffer and then fractionated into detergent-soluble and -insoluble fractions by centrifugation (see Materials and Methods). Analyzing the detergent-insoluble fractions obtained from extracts of unstressed and stressed cells, ANG and RNH1 were slightly enriched in the fractions from SA-stressed cells, as well as TIA-1, a RNA-binding protein that promotes SGs assembly (Figure 3.7). Thus, these data suggested that under stress RNH1 and ANG move to the SGs.

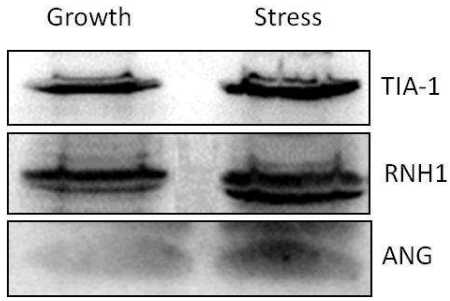

Figure 3.7 Detection of ANG and RNH1 in SGs by Western blot analysis. TIA-1, RNH1 and ANG in NP-40-resistant fractions extracted from HeLa cells cultured in growth and SA-induced stress conditions.

3.4 Localization of ANG and RNH1 in cells recovered from stress

Since SGs are dynamic structures into the cell, able to dissolve them when cell overcomes stress conditions, it has chosen to assess whether the recruitment of both proteins on SGs was reversible under stress recovery conditions.

HeLa cells stressed with 0.5 mM SA for 1 h were then allowed to recover in full growth medium for 3 h. The subcellular localization of ANG and RNH1 in stress recovered cells was at first verified by immunofluorescence (Figure 3.8).

Only a very low percent of cells was still characterized by presence of cytoplasmic SGs, marked by PABP, strongly reduced in size, indicating a normal process of progressive disassembling. Then, ANG relocated back to the nucleus, especially in nucleoli and perinuclear region. This is in line with ANG functions to up-regulate rRNA transcription under physiological conditions and capability of the cell to reactivate its biosynthetic apparatus. Although both proteins were still present in some few granules, RNH1 seems regained its subcellular localization in a greater extent than ANG, the latter found in a slightly higher number of SGs.

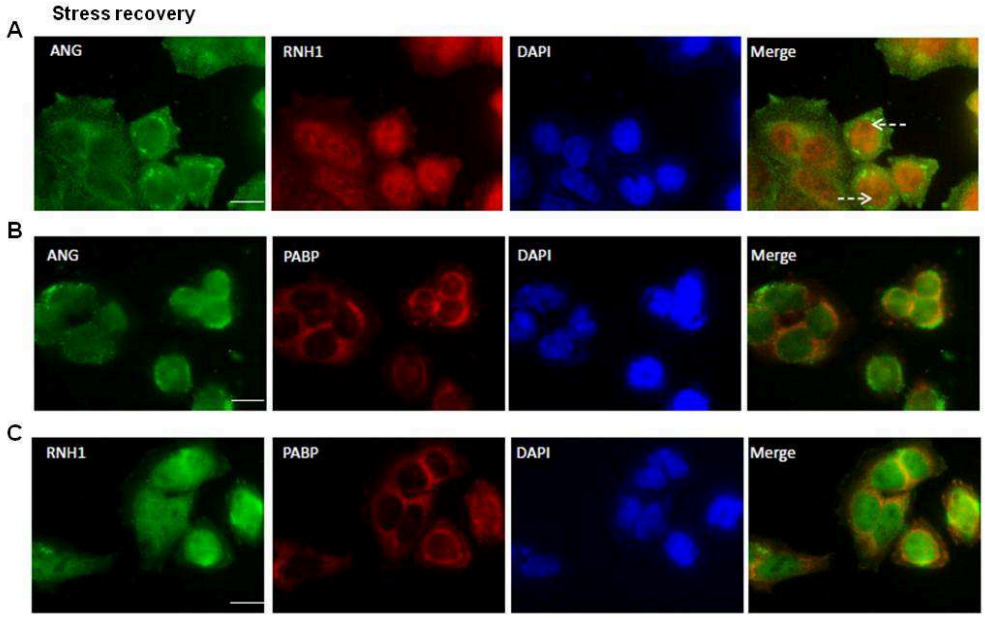

Figure 3.8 Subcellular localization of ANG and RNH1 in HeLa cells recovered from oxidative stress. Stress recovery was obtained by fresh medium exchange and subsequent cell growth for 3 h. Double IF of ANG and RNH1 (A), of ANG and PABP (B) and of RNH1 and PABP (C). Dashed arrows indicate nucleoli. Scale bar, 10 μm.

In order to confirm the data obtained, an alternative approach was carry out based on fractionating in a sucrose gradient of HeLa cytoplasmic extracts, cultured in growth, stress, and in stress recovery conditions. The separation of cellular compartments was achieved by ultracentrifugation, following the fate of both ANG and RNH1 by western blotting analysis of individual gradient fractions (Figure 3.9). Similarly to the data obtained from gel filtration chromatography, in the high molecular weight region the UV absorbance profile at 260 nm (Figure 3.9A) was higher than that one generated by the fractions of unstressed cells. The profile from stress-recovered cells was very similar to that from the cells cultured under growth conditions.

RNH1 and ANG were detected in the lower molecular weight fractions, under growth conditions (Figure 3.9B, first and second panel from the top). Under SA-induced stress conditions RNH1 and ANG moved from low- to high-density gradient regions, i.e. were found in higher molecular weight structures, confirming data obtained by gel filtration chromatography (Figure 3.9B, 4^{th} and 5^{th} panel from top). It is of significant interest to note that ANG and RNH1 were again found in lower molecular weight fractions in the stress recovered cells (Figure 3.9B, bottom 3 panels). So the stress recover process is accompanied by a dynamic movement of ANG and RNH1 into the cell, suggesting that both proteins regain their original localization and probably also their function as well as observed under physiological conditions.

In order to confirm, also in this experiment, that both ANG and RNH1 were organized in high molecular structures like SGs, it was used PABP and RPS3 as SGs markers in Western blot analysis. Under growth conditions, PABP was evenly distributed in the cytoplasm, since that it is notable an almost equal density in every fraction (Figure 3.9B, third panel from top). In stressed cells, PABP was more abundant in fractions 3-11 (Figure 3.9B, 6^{th} panel from top), and RPS3 is particularly accumulated in fractions 5 and 7, indicating that in these fractions SGs were eluted. In stressed cells allowed to recover, PABP level in fractions 3-11 was strongly decreased, showing a almost equal distribution into the cytoplasm, albeit in the fractions 3-5 the intensity was slightly higher, indicating that some granules may still be present in some cells.

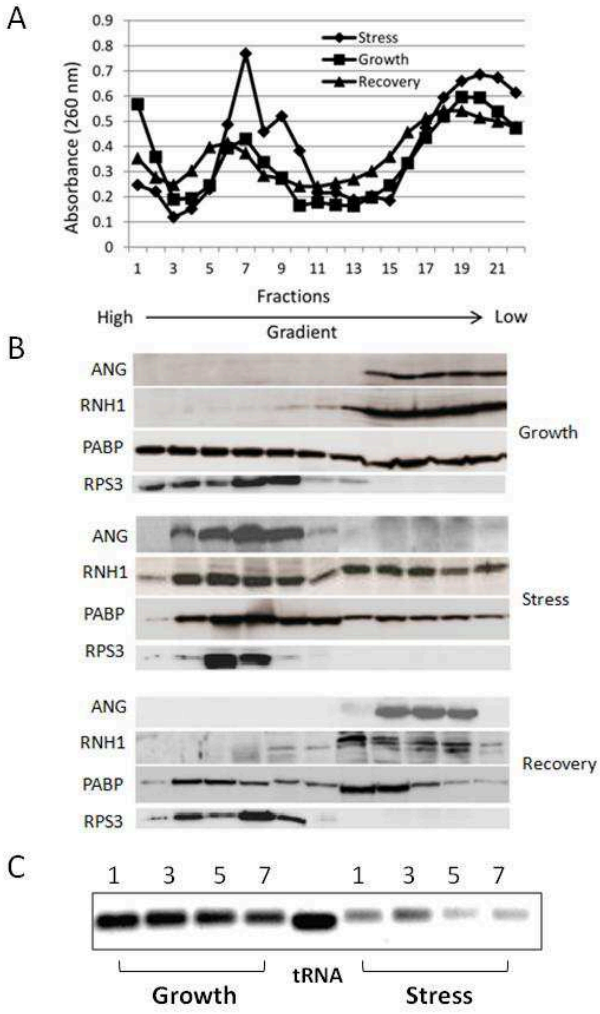

Figure 3.9 Subcellular fractionation by ultra-centrifugation of cytoplasmic extracts in a sucrose gradient. (A) Absorbance profiles at 260 nm of the sucrose gradient fractions (60% to 15%). (B) Western blot analyses of ANG, RNH1, and PABP and RPS3 from alternate gradient fractions collected shown in (A). (C) A ribonucleolytic activity assay in vitro was performed, using yeast tRNA as substrate, on fractions 1-3-5-7 from sucrose gradient eluate.
HeLa cells were cultured under growth and oxidative stress conditions (0.5 mM SA, 1 h). Stress recovery was obtained by fresh medium exchange and subsequent cell growth for 3 h.

It is known that ANG is able to perform tRNA cleavage promoting tiRNAs production and thus the arrest of protein synthesis, under stress conditions. To this regard representative fractions from sucrose gradient eluate (fractions 1-3-5-7), containing ANG and presumably SGs as PABP and RPS3 immuno-detection had revealed (Figure 3.9B, 5^{th} 7^{th} and 8^{th} panels from top), were analyzed. A ribonucleolytic activity assay in vitro was performed, using yeast tRNA as substrate. The same fractions relative to extracts of HeLa cells cultured in growth conditions represented negative control. Actually, cytpolasmic ANG under stress conditions was found to be fully active as detected by agarose gel analysis (Figure 3.9C).

3.5 Interaction between ANG and RNH1

To clarify whether there is an interaction between ANG and RNH1 in the cytoplasm under physiological conditions that actually dissolves under stress conditions, particularly in SGs, immuno-FRET experiments were performed, as an accurate experimental approach used for quantitative determination of molecular proximity and intermolecular interactions.

HeLa cells cultured under growth and SA-induced stress conditions were treated as described above in IF experiments. RNH1 pAb and ANG mAb and relatives red and green fluorescent secondary antibodies were used, respectively. Particularly, Cy3 was the acceptor fluorophore (RNH1) and Alexa Fluor 488 (ANG) was the donor fluorophor. As shown in Figure 3.10, under growth conditions, at the initial time point both fluorescence signals generated by ANG and RNH1 were detected. In the marked region of interest (ROI, marked by a green box in Figure 3.10) in the cytoplasm, the intensity of green fluorescence from the donor was 29.3 ± 7.2 units and that of the red fluorescence from the acceptor was 76.4 ± 3.5 units, respectively. After photobleaching of acceptor red fluorescence (RNH1) to 5.3 ± 0.4 units (6.9% of the original), in the above mentioned ROI, an increase the intensity of the donor fluorescence (ANG) to 32.0 ± 7.6 units was verified. An increase of intensity of fluorescence at 10.1 ± 1.2%, achieved repeating 10 times the experiment, clearly indicated an energy transfer from donor fluorophore to acceptor fluorophore suggesting that a physical interaction between ANG and RNH1 existed in the cytoplasm under physiological conditions. ANG activity in the cytoplasm might be regulated by linking to RNH1 and the existence of the complex could thus prevent random RNA cleavage. Instead, evaluating intensity of fluorescence after photobleaching in selected SGs no energy transfer was observed (Figure 3.10). The fluorescence intensity of the donor was 75.4 ± 9.1 and 76.0 ± 9.6 units, respectively, before and after photobleaching of the acceptor, representing a mere 0.8% increase. Although

ANG and RNH1 are located in SGs, interestingly, they are not physically associated. Therefore, under SA-induced stress conditions cytoplasmic ANG seems be RNH1 free in SGs, being thus able to execute its ribonucleolytic activity to generate tiRNAs and promote cell survival.

To substantiate the relationship between RNH1 and ANG in different subcellular locations and under different growth conditions, co-immunoprecipitation (co-IP) experiments have been performed. Cytoplasmic and nuclear extracts of the cells cultured under growth and SA-induced stress conditions were precipitated by ANG monoclonal antibody (mAb) 26-2F (Figure 3.11A) and by RNH1 affinity-purified polyclonal antibody (pAb) R127 (Figure 3.11B).

Under growth conditions it is notable that ANG and RNH1 did not interact in nuclear fraction, so that ANG biological activity is not inhibited by RNH1 and it is able to stimulate rRNA transcription and promote cell growth. Unlike it is showed that cytoplasmic ANG was associated with RNH1: its ribonucleolytic activity is inhibited to avoid random RNA degradation, deleterious for the cell. When the cells were cultured in SA-induced stress conditions, the remaining nuclear ANG was associated with RNH1, whereas in cytoplasmic fraction no interaction was detected. This is consistent with ANG function in stress conditions to actuate the production of tiRNAs and promote cell survival; in addition it is needed that remaining nuclear ANG is inhibited to reduce rRNA transcription and save anabolic energy. These data are in line with FRET experiments results described in Figure 3.10.

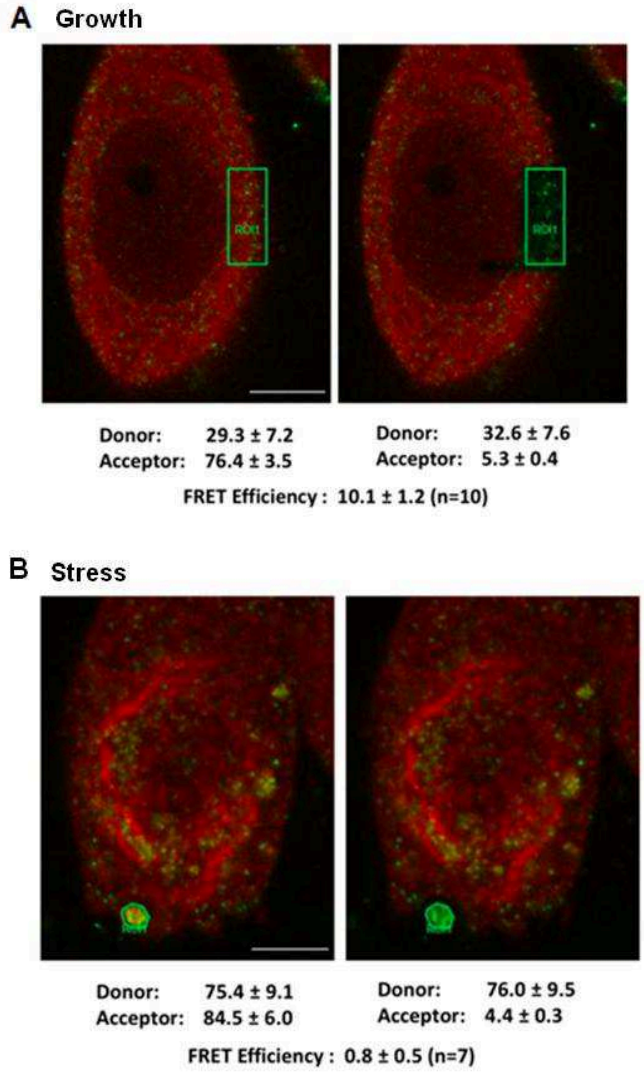

Figure 3.10 FRET analysis on HeLa cells between cytoplasmic ANG and RNH1. HeLa cells were cultured in growth conditions (A) and treated with 0.5 mM SA for 1 h (B). ANG and RNH1 were detected with mAb 26-2F and pAb R127, respectively, and were visualized with Alexa488-labeled goat anti-mouse $F(ab')_2$ and Cy3-labeled goat anti-rabbit $F(ab')_2$. The intensity of both green (donor, ANG) and red (acceptor, RNH1) fluorescence in the selected ROI was recorded both before and after red fluorescence bleaching at 592 nm for 5 s. Data shown are the means ± SD of the intensities of 10 (A) and 7 (B) selected regions. Scale bar, 5 µm.

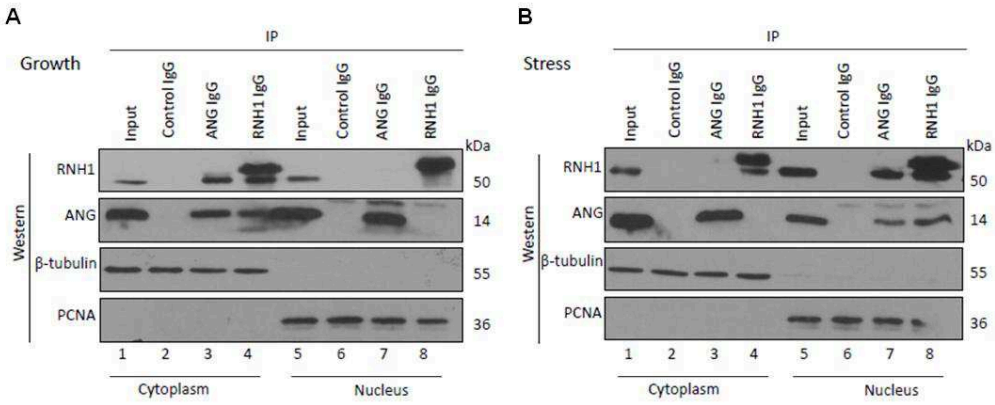

Figure 3.11 Interaction between ANG and RNH1 in the nucleus and cytoplasm. HeLa cells were cultured under growth (A) and stress conditions (B). Stress was realized using 0.5 mM SA for 1h. Cells were fractionated and the cytoplasmic (left 4 lanes of each panel) and nuclear fractions (right 4 panels of each panel) were precipitated with a non-immune mouse IgG, ANG mAb 26-2F, or affinity-purified RNH1 pAb R127. Input control lanes had 10% of the materials used for co-IP. The purity of cytoplasmic and nuclear fractions was analyzed by Western blot analyses of β-tubulin and PCNA.

3.6 Knockdown of RNH1 impairs localization of ANG in SGs and alters cell growth and survival behaviors

To evaluate the effect of RNH1 on regulation of ANG activity and its localization on SGs, RNH1 depletion was performed using small hairpin RNA (shRNA) (see Materials and Methods). Five individual clones representing siRNAs against RNH1 and cloned in lentivirus-mediated shRNA were selected to knockdown RNH1 expression. HeLa cells were transfected with lentivirus encoding a scramble shRNA, RNH1-specific shRNA 33, 34, 35, 36 and 37 and corresponding cytoplasmic extracts were analyzed. Four among five different constructs specifically diminished the expression of the target RNH1, as shown by Western blotting analysis (Figure 12A). Particularly, RNH1-specific shRNA 35 (Sh35) efficiently reduced RNH1 expression with 97% decrease in RNH1 protein level, and it was selected for further studies. The relative intensity of RNH1 was normalized to β-tubulin.

Then it was analyzed whether silencing of RNH1 affected ANG localization in SA-induced stress conditions, examining by IF scramble control and Sh35 transfected HeLa cells. RNH1 knockdown did not disrupted SGs formation, as indicated by PABP immunodetection (Figure 3.12C, second panel), but no ANG was found to be colocalized with PABP (Figure 3.12C, right panel). Also very intriguingly, it was a higher nucleolar localization of ANG as shown in Figure 3.12C (indicated by arrows). Scramble shRNA transfected cells were used as control and the results were not different from that shown by untransfected HeLa cells, in which ANG was localized in SGs (Figure 3.12B).

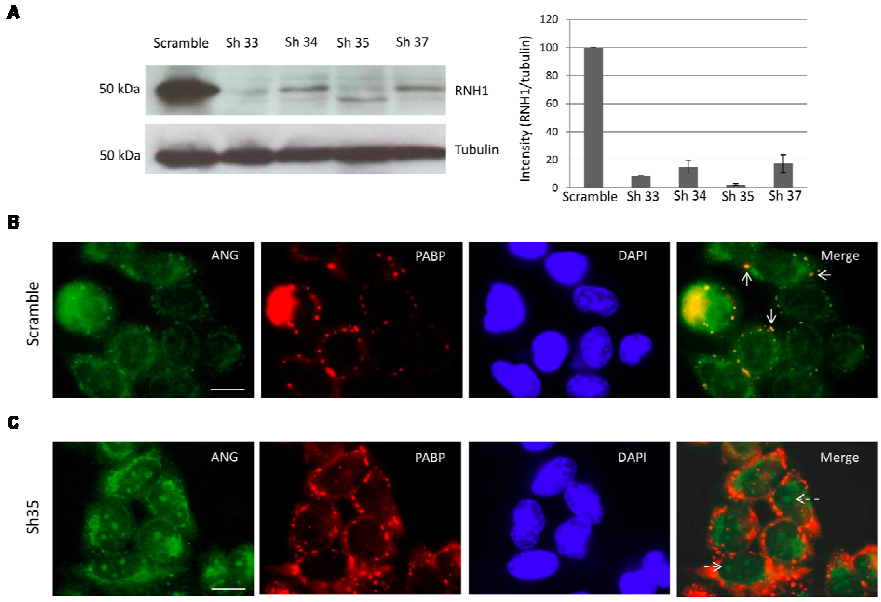

Figure 3.12 RNH1 Knockdown alters subcellular localization of ANG under stress. Knockdown of RNH1 in HeLa cells infected with pLKO.1 lentiviral particles encoding RNH1-specific shRNA and scramble control. (A) RNH1 levels in scramble control and specific RNH1 knockdown HeLa cells. Left panel, Western blot analyses of RNH1 and β-tubulin. Right panel, quantitative analysis by image J of relative band intensity of RNH1 over β-tubulin. (B, C) Subcellular localization of ANG in RNH1 knockdown cells (C) and scramble control cells (B) under oxidative stress (0.5 mM SA 1h). Arrows indicate colocalization of ANG and PABP in scramble control infected cells. Dashed arrows indicate nucleoli staining of ANG in RNH1 knockdown cells. Scale bar, 10 μm.

So stress-induced relocalization of ANG in SGs was impaired permitting instead nucleolar accumulation when RNH1 was down-regulated.

The significance of the subcellular redistribution of ANG in RNH1 knockdown cells under stress is unknown at present. However RNH1 seems regulate ANG movement into the cell.

The consequence of ANG nucleolar accumulation in RNH1 knockdown cells under stress is unclear at present. Thus, it was intriguing estimate whether cell proliferation was enhanced as a result of RNH1 knockdown. Moreover, RNH1 is located on the chromosome 11p15.5, near location of proto-oncogene ras, and recent studies indicate that more than one locus at 11p15 could be involved in tumorigenesis (Chen et al., 2011). Then RNH1 seems interact with PTEN a tumor suppressor by negatively regulating Akt/PKB pathway, mutated in a large number of cancers and target of oncomir miR21. These data suggest that RNH1 may be directly involved in cell growth and differentiation so that it was chosen to execute a proliferation assay through direct cell count. Cell proliferation in RNH1 knockdown cells has been significantly reduced as compared with scramble control (Figure 3.13A), suggesting that the role of nucleolar ANG is context dependent. RNH1 knockdown actually inhibited cell proliferation in a manner closely correlated with the extent of gene expression silencing. Particularly, Sh35 induced a decrease of 31% in cell proliferation in transfected HeLa cells after 48 hours, and 44% after 72 hours.

Cell proliferation was evaluated also in stress response, assaying different doses of SA and 0.5 mM SA at different times. There was a clear death effect with 0.5 mM SA treatment only for 4 hours in Sh35 knock down cells in respect with scramble control cells (Figure 3.13B). The numbers of viable cells in scramble and Sh35 transfectants were 57 and 26%, respectively, of that before the treatment (Figure 3.13B). When the SA concentration was increased to 1 mM, a decrease of cell viability was already visible after 1 h treatment (Figure 3.13C). The numbers of viable cells in scramble and Sh35 transfectants were 81 and 60%, respectively (Figure 3.13C), thus confirming that RNH1 knockdown cells were more sensitive than the scramble control cells. Massive cell death occurred in both scramble and Sh35 transfectants increasing SA concentration at 2 mM (Figure 3.13C). Again, scramble control cells showed a higher cell viability, than RNH1 knockdown cells, characterized by 15% and 9% of viable cells, respectively.

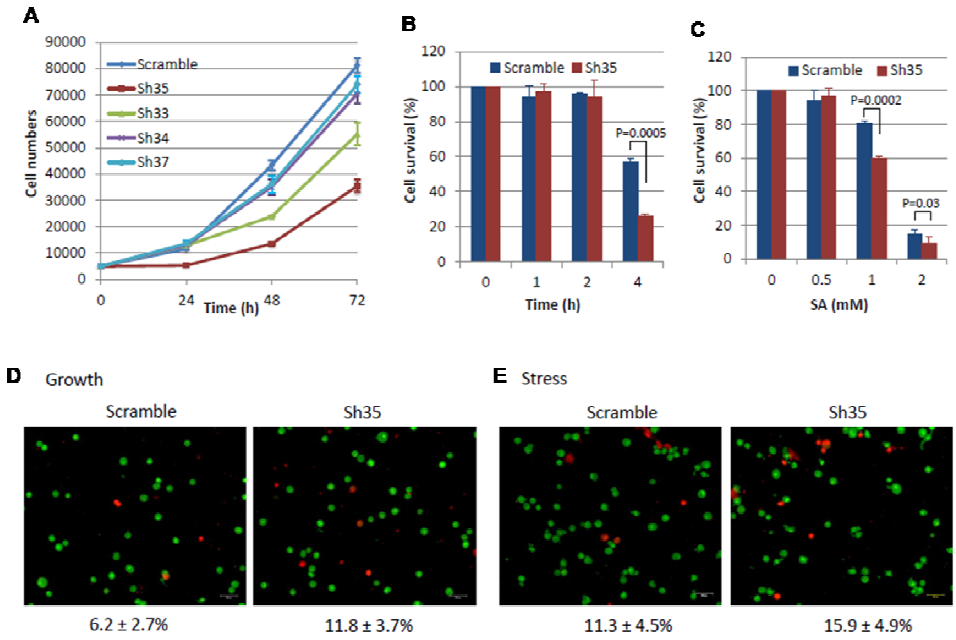

Figure 3.13 RNH1 Knockdown in HeLa cells reduces growth and increases sensitivity to stress. (A) Cell growth of stable scramble and RNH1 shRNA transfectants. Data shown are the means ± SD of 2 separate experiments with triplicates at each data point. (B) Time course of cell survival. Scramble and Sh35 transfectants were cultured in growth medium for 48 h, and then subjected to treatment with 0.5 mM SA for the indicated time. (C) SA dose response of cell survival. Cells were cultured in growth medium for 48 h and treated with different concentrations of SA for 1h. (B, C) Data shown are the means ± SD of triplicates of a representative experiment.
(D) Cell apoptosis under growth conditions. Scramble and Sh35 transfectants were stained with EB/AO. Both apoptotic (red) and live (green) cells were counted. The numbers shown beneath the images were the means ± SD of the percentage of apoptotic cells counted in five microscopic fields.
(E) SA-induced apoptosis. Scramble and Sh35 transfectants were treated with 1 mM SA for 1h and stained with EB/AO. The percentage of apoptotic cells was determined as described in (D).

Taken together, these results indicate that RNH1 knockdown changes ANG localization as well as cell growth and survival, suggesting that a proper RNH1 level may be essential for the cellular functions of ANG.

To determine whether decreased cell proliferation was due to a increased level of cell apoptosis, an ethidium bromide and acridine orange (EB/AO) staining assay was performed to detect and quantify apoptotic cells. AO is a nucleic acid selective fluorescent dye that permeates all cells and staining the nuclei green, while EB is only taken up by cells when cytoplasmic membrane integrity is compromised determining a red staining of the apoptotic nuclei (Ribble et al., 2005). Cell apoptosis level was significantly increased in RNH1 knockdown cells when they were cultured under normal growth conditions as compared to scramble control cells (Figure 3.13D). The percentage of apoptotic cells in Sh35 transfectants was 11.8 ± 3.7%, which is 1.9-fold of that in scramble control transfectants (6.2 ± 2.7%) (Figure 3.13D). When the cells were treated with 1 mM SA for 1 h, the percentage of apoptotic cells in Sh35 and scramble transfectants were 15.9 ± 4.9% and 11.3 ± 4.5%, respectively (Figure 3.13E), representing a 41% increase in SA-induced apoptosis when RNH1 was knocked down. So increased apoptosis may explain decreased growth and survival in RNH1 knockdown cells.

4. Discussion/Conclusions

4.1 Dynamic cellular localization of ANG and RNH1

ANG and RNH1 subcellular localization is dynamic and dependent on the growth status of the cell. Under growth conditions ANG is mainly localized in the nucleus, in line with ANG function in promoting rRNA transcription and stimulate accordingly cell proliferation. Indeed ANG needs to bind to the promoter region of rDNA to induce rRNA transcription. Following stress exposure as oxidative stress (Figures 3.1A, 3.2B and 3.3), heat shock or ER stress (Figure 3.4) a shift of ANG localization from nucleus to cytoplasm occurs. ANG is known to mediate tiRNAs production in the cytoplasm by tRNAs cleavage in adverse conditions and to stimulate cell survival (Yamasaki et al., 2009). The production of tiRNAs suppresses protein synthesis but does not alter IRES-mediated translation. There are several potential mechanisms by which tiRNAs could inhibit mRNAs translation such as associate to unknown general repression complexes or to Argonaute complexes (Thompson and Parker, 2009). It is also note that 5' tiRNAs promote the assembly of SGs by eIF2α phosphorilation-independent pathway (Emara et al., 2010). General protein synthesis inhibition is consistent with cellular stress response, to save anabolic energy needed to the cell for survival and activation of repair pathways. Moreover, in the present study it has been first reported that ANG is localized in stress granules (SGs). It therefore makes sense for ANG to leave nucleus, under adverse environmental conditions, to promote cell survival by tRNAs cleavage and at the same time to avoid unnecessary rRNA production. So differential subcellular localization of ANG under different growth conditions might be a way to regulate its growth-stimulating and pro-survival functions.

Concerning RNH1 subcellular localization, its pattern is opposite to ANG. In this study RNH1 has been found to be mainly located in the nucleus under growth conditions, but not in nucleoli (Figure 3.2A). Under growth conditions, RNH1 is not associated with ANG as shown by co-IP experiments (Figure 3.11A), so that nuclear function ANG in stimulating rRNA transcription is not inhibited. On the contrary, small amount of cytoplasmic ANG is fully associated with RNH1, as shown by both co-IP (Figure 3.11A) and FRET (Figure 3.10A) experiments, so that it is conceivable to hypothesize that its ribonucleolitical activity is completely inhibited. ANG/RNH1 complex formation might be useful to prevent unfavorable RNA degradation in the cytoplasm to maintain a proper healthy status of the cell. Under stress conditions, a higher nuclear RNH1 level is detected (Figures 3.1B and 3.2B). Data obtained from co-IP experiments

(Figure 3.11B) have been showed that in stressed cells ANG and RNH1 are associated in the nuclear fraction. At the same time the stress reduces the amount of cytoplasmic RNH1. Also, its interaction with ANG is impaired as shown by the co-IP experiments (Figure 3.11B). Particularly, exposure to stress also induces RNH1 recruiting to SGs, here first reported. Surprisingly, FRET analysis has revealed that although both RNH1 and ANG colocalize in some SGs, they are not physically associated in SGs (Figure 3.10B). From a functional point of view, it is reasonable to image that under stress cytoplasmic RNH1 dissociates from ANG, so that free ANG is able to perform its ribonucleolytic activity producing tiRNA and thus promoting cell survival.

The mechanism by which RNH1 dissociates from ANG under stress is unknown at present. However, it is note that RNH1 is sensitive to oxidation, likely due to its high content of cysteine residues (Cys). RNH1 contains 32 free Cys and disulfide bonds formation prevents binding to ribonucleases (RNases), drastically altering the 3D structure of RNH1 and greatly increasing its susceptibility to proteasomal degradation (Fominaya and Hofsteenge, 1992).

RNH1 is one of the most abundant cellular proteins (Haigs et al., 2003): its biochemical features have been well documented including x-ray structures of both free RNH1 and in complex with some RNases such as ANG. Compared to the well-defined biochemical properties of RNH1, knowledge of its functional roles is evolving. Cytoplasmic RNH1 is mainly known to inhibit RNases such as ANG, or to be involved in cellular redox homeostasis through its high content in Cys. Recent studies have reported a new role of nuclear RNH1. It has been shown that RNH1 is necessary and sufficient for pri-miR-21 processing, through a direct interaction with the RNase III Drosha (Kim et al., 2011). Indeed, importantly, RNH1 contains 15 leucine-rich repeats (LRRs), usually essential in the formation of protein-protein interactions. So RNH1 might interact with PTEN or Drosha complex, or even pri-miR-21, through the LRRs for an efficient miRNAs processing.

Besides nuclear RNH1 functions are still not totally defined, it remains unclear how RNH1 subcellular localization, especially nuclear shuttling, could be regulated. At this regard it should be noted that its molecular weight is 50 kDa, a limit size for diffusion by nuclear pores, and a specific nuclear localization signal (NLS) has not still identified. It could be hypothesized for RNH1 a subcellular trafficking mechanism similar to that proposed for PTEN, with which RNH1 shares some structural features. For example, PTEN does not also have a functional NLS sequence and it mediates its different functions through protein-protein interactions. It has

been demonstrated that mono-ubiquitination regulates PTEN nuclear import necessary for its activity while poly-ubiquitination results in its cytoplasmic retention and degradation. Nuclear PTEN ubiquitinated can shuttle back to the cytoplasm or after de-ubiquitination can be retained into nucleus and protected from cytoplasmic degradation until it is again mono-ubiquitinated and exported (Trotman et al., 2007). Immunoprecipitation and mass spectrometry data for RNH1, have shown for RNH1 an interaction with E3 ubiquitin protein ligase and ubiquitin carboxyterminal hydrolase (a deubiquitinating enzyme), so that a mechanism based on ubiquitination could be suggested to regulate nuclear import and export of RNH1.

The elucidation of the mechanisms of nuclear translocation of RNH1 could provide new insights about its cell functional properties under physiological and pathological conditions.

4.2 RNH1 regulates ANG localization in SGs under stress and cell proliferation and survival behaviors

Stress induces recruitment of both RNH1 and ANG in SGs (Figures 3.6 and 3.7). SGs are primarily composed of the stalled 48S pre-initiation complexes containing mRNAs bound to small ribosome subunits, initiation factors eIF4E, eIF3, eIF4A, eIF4G, and PABP (Anderson and Kedersha, 2008). Over these core components, SGs also contain other proteins with diverse functions including RNA-binding proteins, RNA helicases, nucleases, kinases and SG-associated signaling molecules that rapidly shuttle in and out of SGs (Anderson and Kedersha, 2009). ANG has been detected in almost all SGs induced by sodium arsenite (SA) (Figure 3.6C). On the contrary, RNH1 has been found only in some but not all SA-induced SGs (Figure 3.6D). In SGs that contained both ANG and RNH1, ANG is not associated with RNH1 as shown by FRET experiments (Figure 3.10B). Therefore, cytoplasmic ANG that is localized in SGs would be ribonucleolytically active.

The mechanisms by which ANG and RNH1 are recruited to SGs and their functions in SGs are unknown. Some data obtained from immunoprecipitation and mass spectrometry experiments have evidenced some RNH1 partners that can be traced back to SGs. For example, a potential partner of RNH1 is 40S ribosomal protein S3, a core component of SGs; another putative partner is HSP70, an essential molecule required to release mRNAs from SGs for their storage o re-initiation and to reverse the aggregation of SGs core proteins. However, localization of an active ribonuclease or in any case of RNA-regulatory proteins in SGs where both RNA and ribonucleoproteins exist should not be merely by chance.

It is of particular interest to note that SGs also contain RNA-induced silencing complexes (RISCs). It is known that RNH1 mediates oncogenic miR-21 biogenesis, although it remains to be determined whether RNH1 regulates the processing of other miRNAs. It is conceivable hypothesize that the function of ANG and RNH1 located in SGs may be integrated with microRNA-induced translational silencing mechanism. Therefore, ANG and RNH1 might play a role in micro RNA metabolism and that SG may be an additional or alternative place where micro RNA are generated or metabolized.

Moreover, ANG localization in SGs is strongly compromised in RNH1 knockdown cells, following SA treatment. At the same time an ANG nucleolar accumulation is instead promoted. The consequence of ANG nucleolar re-distribution in RNH1 knockdown cells under stress is unclear at present. Nevertheless, the results collected in the present study clearly indicate that RNH1 influences and regulates ANG subcellular localization.

RNH1 knockdown actually inhibited cell proliferation in a dose-dependent manner. Under growth conditions there is a positive corresponding between RNH1 knockdown extent and reduced viable cells number (Figure 3.13A). One of the reasons for decreased growth in RNH1 knockdown cells can be attributed to increased apoptosis. The percent of apoptotic cells almost doubles in RNH1 knockdown cells (Figure 3.13D). Under stress conditions, survival of RNH1 knockdown cells is also significantly decreased (Figure 3.13B and 3.13C), accompanied again with an increase in cell apoptosis (Figure 3.13E). Various could be the reasons for which a decreased survival of RNH1 knockdown cells occurs in oxidative stress conditions. The abnormal ANG cellular localization (Figure 3.12C) in nucleoli but not in SGs when RNH1 knockdown cells are exposed to SA stress might be one explanation. On the one side, since rRNA transcription is an energetically costly process, it is counterproductive for the stressed cell that nucleolar ANG continually produces rRNA. On the other side, failure of ANG to localize in SGs could prevent a stress response pathway by tiRNAs production. Moreover, the proposed roles as ROS scavenger (Cui et al., 2003) and as redox homeostasis controller (Monti et al., 2007) may also contribute to the regulatory function of RNH1 in cell survival.

6. References

Abernathy, C. O., Liu, Y. P., Longfellow, D., Aposhian, H. V., Beck, B., Fowler, B., Goyer, R., Menzer, R., Rossman, T., Thompson, C., and Waalkes, M. (1999). Arsenic: health effects, mechanisms of actions, and research issues. Environ Health Perspect *107***,** 593–597.

Anderson, P. and Kedersha, N. (2002). Stressful initiations. Journal of Cell Science *115*, 3227-3234.

Anderson, P., and Kedersha, N. (2006). RNA granules. J Cell Biol *172*, 803-808.

Anderson, P., and Kedersha, N. (2008). Stress granules: the Tao of RNA triage. Trends Biochem Sci *33*, 141-150.

Anderson, P. and Kedersha, N. (2009). RNA granules: post-transcriptional and epigenetic modulators of gene expression. Nature Rev Mol Cell Biol *10*, 430-436.

Baird, S. D., Turcotte, M., Korneluk, R. G., and Holcik, M. (2006). Searching for IRES. RNA *12*, 1755-1785.

Bella, J., Hindle, K.L., McEwan, P.A., Lovell, S.C. (2008). The leucine-rich repeat structure. Cell Mol Life Sci *65***,** 2307–2333.

Blackburn, P., Wilson, G., and Moore, S. (1977). Ribonuclease inhibitor from human placenta. Purification and properties. J Biol Chem *252*, 5904-5910.

Blázquez, M., Fominaya, J.M., and Hofsteenge, J. (1996). Oxidation of sulfhydryl groups of ribonuclease inhibitor in epithelial cells is sufficient for its intracellular degradation. J Biol Chem *271*, 18638-18642.

Botella-Estrada, R., Malet, G., Revert, F., Dasi, F., Crespo, A., Sanmartin, O., Guillen, C., and Alino, S. F. (2001). Antitumor effect of B16 melanoma cells genetically modified with the angiogenesis inhibitor rnasin. Cancer Gene Ther *8*, 278-284.

Buchan, J.R., and Parker, R. (2009). Eukaryotic stress granules: the ins and outs of translation. Mol Cell *36*, 932-941.

Chen, J., Ou-Yang, X., Gao, J., Zhu, J., He, X., and Rong, J. (2011). Knockdown of ribonuclease inhibitor expression with siRNA in non-invasive bladder cancer cell line BIU-87 promotes growth and metastasis potentials. Mol Cell Biochem *349*, 83-95.

Chen, J. X., Gao, Y., Liu, J. W., Tian, Y. X., Zhao, J., and Cui, X. Y. (2005). Antitumor effects of human ribonuclease inhibitor gene transfected on B16 melanoma cells. Int J Biochem Cell Biol *37*, 1219-1231.

Conforti, F. L., Sprovieri, T., Mazzei, R., Ungaro, C., La Bella, V., Tessitore, A., Patitucci, A., Magariello, A., Gabriele, A. L., Tedeschi, G.*, et al.* (2008). A novel Angiogenin gene mutation in a sporadic patient with amyotrophic lateral sclerosis from southern Italy. Neuromuscul Disord *18*, 68-70.

Cui, X. Y., Fu, P. F., Pan, D. N., Zhao, Y., Zhao, J., and Zhao, B. C. (2003). The antioxidant effects of ribonuclease inhibitor. Free Radic Res *37*, 1079-1085.

D'Alessio, G. and Riordan, J.F. (1997). Ribonucleases: Structures and Functions. Academic Press, San Diego.

Dickson, K.A., Haigis, M.C., and Raines, R.T. (2005). Ribonuclease inhibitor: structure and function. Prog Nucleic Acid Res Mol Biol *80*, 349-374.

Emara, M.M., Ivanov, P., Hickman, T., Dawra, N., Tisdale, S., Kedersha, N., Hu, G.F., and Anderson, P. (2010). Angiogenin-induced tiRNAs promote stress-induced stress granule assembly. J Biol Chem *285*, 10959-10968.

Fett, J. W., Strydom, D. J., Lobb, R. R., Alderman, E. M., Bethune, J. L., Riordan, J. F., and Vallee, B. L. (1985). Isolation and characterization of angiogenin, an angiogenic protein from human carcinoma cells. Biochemistry *24*, 5480-5486.

Fominaya, J. M., and Hofsteenge, J. (1992). Inactivation of ribonuclease inhibitor by thiol-disulfide exchange. J Biol Chem *267*, 24655-24660.

Fu, H., Feng, J., Liu, Q., Sun, F., Tie, Y., Zhu, J., Xing, R., Sun, Z., and Zheng, X. (2009). Stress induces tRNA cleavage by angiogenin in mammalian cells. FEBS Lett *583*, 437-442.

Furia, A., Moscato, M., Cali, G., Pizzo, E., Confalone, E., Amoroso, M. R., Esposito, F., Nitsch, L., and D'Alessio, G. (2011). The ribonuclease/angiogenin inhibitor is also present in mitochondria and nuclei. FEBS Lett *585*, 613-617.

Gao, X., and Xu, Z. (2008). Mechanisms of action of angiogenin. Acta Biochim Biophys Sin *40*, 619-624.

Greenway, M. J., Andersen, P. M., Russ, C., Ennis, S., Cashman, S., Donaghy, C., Patterson, V., Swingler, R., Kieran, D., Prehn, J.*, et al.* (2006). ANG mutations segregate with familial and 'sporadic' amyotrophic lateral sclerosis. Nat Genet *38*, 411-413.

Haigis, M. C., Kurten, E. L., and Raines, R. T. (2003). Ribonuclease inhibitor as an intracellular sentry. Nucleic Acids Res *31*, 1024-1032.

Hofsteenge, J. (1997). Ribonuclease inhibitor. In: Ribonucleases: Structures and Functions, eds. G. D'Alessio and J.F. Riordan, 621-658. Academic Press, San Diego.

Hu G. F., Riordan J. F., and Vallee B. L. (1997). Proc. Natl. Acad. Sci. U S A *94*, 2204–2209.

Ibaragi, S., Yoshioka, N., Kishikawa, H., Hu, J. K. Sadow, P. M. Li, M., and Hu, G. F. (2009). Angiogenin-Stimulated rRNA Transcription Is Essential for Initiation and Survival of AKT-Induced Prostate Intraepithelial Neoplasia. Mol Cancer Res *7***,** 415-424.

Ivanov, P., Emara, M. M., Villen, J., Gygi, S. P., and Anderson, P. (2011). Angiogenin-Induced tRNA Fragments Inhibit Translation Initiation. Mol Cell *43*, 613-623.

Ivanov, P., and Anderson, P., (2011). Stress-Induced Ribonucleases. Nucleic Acids and Molecular Biology *26*, 115-134.

Jomova, K., Jenisova, Z., Feszterova, M., Baros, S., Liska, J., Hudecova, D., Rhodes, C. J. And Valko, M. (2011). Arsenic: toxicity, oxidative stress and human disease. J Appl Toxicol *31*, 95-107.

Kedersha, N., Gupta, M., Li, W., Miller, I., and Anderson, P. (1999). RNA-binding proteins TIA-1 and TIAR link the phosphorylation of eIF-2 alpha to the assembly of mammalian stress granules. J Cell Biol *147*, 1431-1442.

Kedersha, N., Cho, M., Li, W., Yacono, P., Chen, S., Gilks, N., Golan, D. and Anderson, P. (2000). Dynamic shuttling of TIA-1 accompanies the recruitment of mRNA to mammalian stress granules. J Cell Biol *151*, 1257-1268.

Kedersha, N., and Anderson, P. (2002). Stress granules: sites of mRNA triage that regulate mRNA stability and translatability. Biochem Soc Trans *30*, 963-969.

Kedersha, N., Stoecklin, G., Ayodele, M., Yacono, P., Andersen, J.L., Fritzler, M. J., Scheuner, D., Kaufman, R.J., Golan, D.E. and Anderson, P. (2005). Stress granules and processing bodies are dynamically linked sites of mRNP remodeling. J Cell Biol *169*, 871-884.

Kieran, D., Sebastià, J., Greenway, M.J., King, M.A., Connaughton, D., Concannon, C.G., Fenner, B., Hardiman, O., Prehn, J.H. (2008). Control of motoneuron survival by angiogenin. J Neurosci *28*, 14056-14061.

Kihlmark, M., and Hallberg, E. (1998). Preparation of nuclei and muclear envelope. In: Cell biology: A laboratory handbook. (J. E. Celis, ed) *2*, 152-158. Academic Press, San Diego.

Kim, Y. J., Park, S. J., Choi, E. Y., Kim, S., Kwak, H. J., Yoo, B. C., Yoo, H., Lee, S. H., Kim, D., Park, J. B., and Kim, J. H. (2011). PTEN modulates miR-21 processing via RNA-regulatory protein RNH1. PLoS One *6*, e28308.

Kim, Y. N., and Kim, D. H. (2012). Decreased serum angiogenin level in Alzheimer's disease. Prog Neuropsychopharmacol Biol Psychiatry *38*, 116-120.

Kimball, S.R., Horetsky, R.L., Ron, D., Jefferson, L.S., and Harding, H.P. (2003). Mammalian stress granules represent sites of accumulation of stalled translation initiation complexes. Am J Physiol Cell Physiol *284*, 273-284.

Kishimoto, K., Liu, S., Tsuji, T., Olson, K. A., and Hu, G. F. (2005). Endogenous angiogenin in endothelial cells is a general requirement for cell proliferation and angiogenesis. Oncogene *24*, 445-456.

Kobe, B., and Deisenhofer, J. (1993). Crystal structure of porcine ribonuclease inhibitor, a protein with leucine-rich repeats. Nature *366*, 751-756.

Kobe, B., and Deisenhofer, J. (1996). Mechanism of ribonuclease inhibition by ribonuclease inhibitor protein based on the crystal structure of its complex with ribonuclease A. J Mol Biol *264*, 1028-1043.

Lee, F.S. and Vallee, B.L. (1989). Expression of human placental ribonuclease inhibitor in Escherichia coli. Biochem Biophys Res Commun *160*, 115-120.

Lee, F.S. and Vallee, B.L. (1989). Binding of placental ribonuclease inhibitor to the active site of angiogenin. Biochemistry *28*, 3556-3661.

Lee, F. S., Shapiro, R., and Vallee, B. L. (1989). Tight-binding inhibition of angiogenin and ribonuclease A by placental ribonuclease inhibitor. Biochemistry *28*, 225-230.

Leland, P. A., Raines, R. T. (2001). Cancer chemotherapy-ribonucleases to the rescue**.** Chem Biol *8*, 405-413.

Li, S., and Hu, G. F. (2010). Angiogenin-mediated rRNA transcription in cancer and neurodegeneration. Int J Biochem Mol Biol *1*, 26-35.

Li, S., Ibaragi, S., and Hu, G. F. (2011). Angiogenin as a molecular target for the treatment of prostate cancer. Curr Cancer Ther Rev *7*, 83-90.

Li, S., and Hu, G. F. (2012). Emerging role of angiogenin in stress response and cell survival under adverse conditions. J Cell Physiol *227*, 2822-2826.

Lindsay A. J., and McCaffrey, M.W. (2011). Myosin Va is required for P body but not stress granule formation. J Biol Chem *286*, 11519-11528.

McEwen, E., Kedersha, N., Song, B., Scheuener, D., Gilks, N., Han, A., Chen, J. J., Anderson, P., and Kaufman, R. J. (2005). Heme-regulated inhibitor kinase-mediated phosphorylation of eukaryotic translation initiation factor 2 inhibits translation, induces stress granule formation, and mediates survival upon arsenite exposure. J Biol Chem *280*, 16925-16933.

McLaughlin, R. L., Phukan, J., McCormack, W., Lynch, D. S., Greenway, M., Cronin, S., Saunders, J., Slowik, A., Tomik, B., Andersen, P. M.*, et al.* (2010). Angiogenin Levels and ANG Genotypes: Dysregulation in Amyotrophic Lateral Sclerosis. PLoS One *5*, e15402.

Miller, W. H., Schipper, H. M., Lee, J. S., Singer, J., Waxman, S. (2002). Mechanisms of action of arsenic trioxide. Cancer Res *62*, 3893-3903.

Monti, D. M., D'Alessio, G. (2004). Cytosolic RNase inhibitor only affects RNases with intrinsic cytotoxicity. J Biol Chem *279*,39195-8.

Monti, D. M., Montesano Gesualdi, N., Matousek, J., Esposito, F., and D'Alessio, G. (2007). The cytosolic ribonuclease inhibitor contributes to intracellular redox homeostasis. FEBS Lett *581*, 930-934.

Moroianu, J., and Riordan, J. F. (1994). Nuclear translocation of angiogenin in proliferating endothelial cells is essential to its angiogenic activity. Proc Natl Acad Sci U S A *91*, 1677-1681.

Muramatsu, M., Smetana, K. And Bush, H. (1963). Quantitative aspects of isolation of nucleoli of the Walker carcinoma and liver of the rat. Cancer Res *25*, 693-697.
Nazar, R. N. (2004). Ribosomal RNA processing and ribosome biogenesis in eukaryotes. IUBMB Life *56*, 457-465.

Papageorgiou, A. C., Shapiro, R., and Acharya, K. R. (1997). Molecular recognition of human angiogenin by placental ribonuclease inhibitor--an X-ray crystallographic study at 2.0 A resolution. EMBO J *16*, 5162-5177.

Olson K.A., Byers H.R., Key M.E., and Fett J.W. (2002). Inhibition of prostate carcinoma establishment and metastatic growth in mice by an antiangiogenin monoclonal antibody. Int J Cancer *98*, 923-929

Ribble, D., Goldstein, N. B., Norris, D. A., and Shellman, Y. G. (2005). A simple technique for quantifying apoptosis in 96-well plates. BMC Biotechnol *5*, 12.

Riordan, J. F. (2001). Angiogenin. Methods Enzymol *341*, 263-273.

Rutkoski, T. J., and Raines, R. T. (2008). Evasion of ribonuclease inhibitor as a determinant of ribonuclease cytotoxicity. Curr Pharm Biotechnol *9*, 185-189.

Saikia, M., Krokowski, D., Guan, B. J., Ivanov, P., Parisien, M., Hu, G. F., Anderson, P., Pan, T., and Hatzoglou, M. (2012). Genome-wide identification and quantitative analysis of cleaved tRNA fragments induced by cellular stress. J Biol Chem *287*, 42708-42725.

Saxena, S. K., Rybak, S. M., Davey, R. T., Jr., Youle, R. J., and Ackerman, E. J. (1992). Angiogenin is a cytotoxic, tRNA-specific ribonuclease in the RNase A superfamily. J Biol Chem *267*, 21982-21986.

Sebastià, J., Kieran, D., Breen, B., King, M.A., Netteland, D.F., Joyce, D., Fitzpatrick, S.F., Taylor, C.T., Prehn, J.H. (2009). Angiogenin protects motoneurons against hypoxic injury. Cell Death Differ *16*,1238-1247.

Shapiro, R., and Vallee, B.L. (1987). Human placental ribonuclease inhibitor abolishes both angiogenic and ribonucleolytic activities of angiogenin. Proc Natl Acad Sci U S A *84***,** 2238-2241.

Shapiro, R., and Vallee, B. L. (1989). Site-directed mutagenesis of histidine-13 and histidine-114 of human angiogenin. Alanine derivatives inhibit angiogenin-induced angiogenesis. Biochemistry *28*, 7401-7408.

Shapiro, R., Ruiz-Gutierrez, M., Chen, C.Z. (2000). Analysis of the interactions of human ribonuclease inhibitor with angiogenin and ribonuclease A by mutagenesis: importance of inhibitor residues inside versus outside the C-terminal "hot spot". J Mol Biol *302***,** 497-519.

Shapiro, R. (2001). Cytoplasmic Ribonuclease Inhibitor. Methods Enzymol *341*, 611-628.

Steidinger, T. U., Standaert, D. G., and Yacoubian, T. A. (2011). A neuroprotective role for angiogenin in models of Parkinson's disease. J Neurochem *116*, 334-341.

Thiyagarajan, N., Ferguson, R., Subramanian, V., and Acharya, K. R. (2012). Structural and molecular insights into the mechanism of action of human angiogenin-ALS variants in neurons. Nat Commun *3*, 1121.

Thomas, M.G., Martinaez Tosar, L.J., Desbats, M.A., Leishman, C.C. and Boccaccio, G.L. (2008). Mammalian Staufen 1 is recruited to stress granules and impairs their assembly. J Cell Sci *122*, 563-573.

Thompson, D. M., Lu, C., Green, P. J., and Parker, R. (2008). tRNA cleavage is a conserved response to oxidative stress in eukaryotes. RNA *14*, 2095-2103.

Thompson, D.M., and Parker, R. (2009). Stressing out over tRNA cleavage. Cell *138*, 215-219.

Thompson, D.M., and Parker, R. (2009). The RNase Rny1p cleaves tRNAs and promotes cell death during oxidative stress in Saccharomyces cerevisiae. J Cell Biol *185*, 43-50.

Trotman, L.C., Wang, X., Alimonti, A., Chen, Z., Teruya-Feldstein, J., Yang, H., Pavletich, N.P., Carver, B.S., Cordon-Cardo, C., Erdjument-Bromage, H., Tempst, P., Chi, S.G., Kim, H.J., Misteli, T., Jiang, X., Pandolfi, P.P. (2007). Ubiquitination regulates PTEN nuclear import and tumor suppression. Cell *128*, 141-156.

Tsuji, T., Sun, Y., Kishimoto, K., Olson, K.A., Liu, S., Hirukawa, S., and Hu, G.F. (2005). Angiogenin is translocated to the nucleus of HeLa cells and is involved in ribosomal RNA transcription and cell proliferation. Cancer Res *65*, 1352-1360.

van Es, M. A., Schelhaas, H. J., van Vught, P. W., Ticozzi, N., Andersen, P. M., Groen, E. J., Schulte, C., Blauw, H. M., Koppers, M., Diekstra, F. P.*, et al.* (2011). Angiogenin variants in Parkinson disease and amyotrophic lateral sclerosis. Ann Neurol *70*, 964-973.

Wang, T., Yang, M., Chen, J., Watkins, T., and Xiuyun, C. (2005). Inhibition of B16 melanoma growth in vivo by retroviral vector-mediated human ribonuclease inhibitor. Angiogenesis *8*, 73-81.

Wang, S., and Li, H. (2006). Radical scavenging activity of ribonuclease inhibitor from cow placenta. Biochemistry *71*, 520-524.

Wessel, D. and Flügge, U. I. (1984). A method for the quantitative recovery of protein in dilute solution in the presence of detergents and lipids. Anal Biochem *138*, 141-143.

Wu, D., Yu, W., Kishikawa, H., Folkerth, R. D., Iafrate, A. J., Shen, Y., Xin, W., Sims, K., and Hu, G. F. (2007). Angiogenin loss-of-function mutations in amyotrophic lateral sclerosis. Ann Neurol *62*, 609-617.

Xu, Z. P., Tsuji, T., Riordan, J. F., and Hu, G. F. (2002). The nuclear function of angiogenin in endothelial cells is related to rRNA production. Biochem Biophys Res Commun *294*, 287-292.

Xu, Z. P., Tsuji, T., Riordan, J. F., and Hu, G. F. (2003). Identification and characterization of an angiogenin-binding DNA sequence that stimulates luciferase reporter gene expression. Biochemistry *42*, 121-128.

Yamasaki, S. and Anderson, P. (2008). Reprogramming mRNA translation during stress. Curr Opin Cell Biol *20*, 222-226

Yamasaki, S., Ivanov, P., Hu, G.F., and Anderson, P. (2009). Angiogenin cleaves tRNA and promotes stress-induced translational repression. J Cell Biol *185*, 35-42.

Yoshioka, N., Wang, L., Kishimoto, K., Tsuji, T., and Hu, G. F. (2006). A therapeutic target for prostate cancer based on angiogenin-stimulated angiogenesis and cancer cell proliferation. Proc Natl Acad Sci U S A *103*, 14519-14524.